Boltzmann hierarchy

Photons

$$\dot{\Delta}^{(S)}_{T,\ell}(q,t) + \frac{q}{a(2\ell+1)}\left[(\ell+1)\Delta^{(S)}_{T,\ell+1}(q,t) - \ell\Delta^{(S)}_{T,\ell-1}(q,t)\right]$$
$$= -\omega_c(t)\Delta^{(S)}_{T,\ell}(q,t) - 2\dot{A}_q\delta_{\ell,0} + 2q^2\dot{B}_q\left(\frac{1}{3}\delta_{\ell,0} - \frac{2}{15}\delta_{\ell,2}\right)$$
$$+\omega_c\Delta^{(S)}_{T,0}\delta_{\ell,0} + \frac{1}{10}\omega_c\Pi\delta_{\ell,2} - \frac{4}{3}\frac{q}{a}\omega_c\delta u_{b\,q}\delta_{\ell,1}$$

$$\dot{\Delta}^{(S)}_{P,\ell}(q,t) + \frac{q}{a(2\ell+1)}\left[(\ell+1)\Delta^{(S)}_{P,\ell+1}(q,t) - \ell\Delta^{(S)}_{P,\ell-1}(q,t)\right]$$
$$= -\omega_c(t)\Delta^{(S)}_{P,\ell}(q,t) + \frac{1}{2}\omega_c(t)\Pi(q,t)\left(\delta_{\ell,0} + \frac{1}{5}\delta_{\ell,2}\right)$$

with source function

$$\Pi = \Delta^{(S)}_{P,0} + \Delta^{(S)}_{T,2} + \Delta^{(S)}_{P,2}$$

Boltzmann hierarchy

Photons

$$\dot{\Delta}^{(S)}_{T,\ell}(q,t) + \frac{q}{a(2\ell+1)}\left[(\ell+1)\Delta^{(S)}_{T,\ell+1}(q,t) - \ell\Delta^{(S)}_{T,\ell-1}(q,t)\right]$$

$$= -\omega_c(t)\Delta^{(S)}_{T,\ell}(q,t) - 2\dot{A}_q\delta_{\ell,0} + 2q^2\dot{B}_q\left(\frac{1}{3}\delta_{\ell,0} - \frac{2}{15}\delta_{\ell,2}\right)$$

$$+\omega_c\Delta^{(S)}_{T,0}\delta_{\ell,0} + \frac{1}{10}\omega_c\Pi\delta_{\ell,2} - \frac{4}{3}\frac{q}{a}\omega_c\delta u_{b\,q}\delta_{\ell,1}$$

$$\dot{\Delta}^{(S)}_{P,\ell}(q,t) + \frac{q}{a(2\ell+1)}\left[(\ell+1)\Delta^{(S)}_{P,\ell+1}(q,t) - \ell\Delta^{(S)}_{P,\ell-1}(q,t)\right]$$

$$= -\omega_c(t)\Delta^{(S)}_{P,\ell}(q,t) + \frac{1}{2}\omega_c(t)\Pi(q,t)\left(\delta_{\ell,0} + \frac{1}{5}\delta_{\ell,2}\right)$$

with source function

$$\Pi = \Delta^{(S)}_{P,0} + \Delta^{(S)}_{T,2} + \Delta^{(S)}_{P,2}$$

Polarization sourced by temperature quadrupole

Equations of motion

(Massless) Neutrinos

$$\dot{\Delta}^{(S)}_{\nu,\ell}(q,t) + \frac{q}{a(2\ell+1)}\left[(\ell+1)\Delta^{(S)}_{\nu,\ell+1}(q,t) - \ell\Delta^{(S)}_{\nu,\ell-1}(q,t)\right] = -2\dot{A}_q\delta_{\ell,0} + 2q^2\dot{B}_q\left(\frac{1}{3}\delta_{\ell,0} - \frac{2}{15}\delta_{\ell,2}\right)$$

Baryons

Energy conservation

$$\delta\dot{\rho}_{b\,q} + \frac{3\dot{a}}{a}\delta\rho_{b\,q} - \frac{q^2}{a^2}\overline{\rho}_b\delta u_{b\,q} + \frac{1}{2}\overline{\rho}_b\left(3\dot{A}_q - q^2\dot{B}_q\right) = 0$$

Momentum conservation

$$\delta\dot{u}_{b\,q} + \frac{4}{3}\frac{\overline{\rho}_\gamma}{\overline{\rho}_b}\omega_c(t)\left(\delta u_{b\,q} + \frac{3}{4}\frac{a}{q}\Delta^{(S)}_{T,1}(q,t)\right) = 0$$

Equations of motion

Dark Matter

$$\delta\dot{\rho}_{c\,q} + \frac{3\dot{a}}{a}\delta\rho_{c\,q} + \frac{1}{2}\overline{\rho}_{c\,q}\left(3\dot{A}_q - q^2\dot{B}_q\right) = 0$$

Scalar metric perturbations

$$\frac{q^2}{a^2}A_q + \frac{\dot{a}}{a}\left(3\dot{A}_q - q^2\dot{B}_q\right) = 8\pi G\left(\delta\rho_{q\,b} + \delta\rho_{q\,c} + \overline{\rho}_\gamma\Delta^{(S)}_{T,0} + \overline{\rho}_\nu\Delta^{(S)}_{\nu,0}\right)$$

$$\dot{A}_q = 8\pi G\left(\overline{\rho}_b\delta u_{b\,q} - \frac{a}{q}\overline{\rho}_\gamma\Delta^{(S)}_{T,1}(q,t) - \frac{a}{q}\overline{\rho}_\nu\Delta^{(S)}_{\nu,1}(q,t)\right)$$

Line-of-sight integration

We can write the Boltzmann equation as

$$\dot{\Delta}_T^{(S)}(q,\mu,t) + i\frac{q\mu}{a(t)}\Delta_T^{(S)}(q,\mu,t) = -\omega_c(t)\Delta_T^{(S)}(q,\mu,t)$$
$$+\omega_c\Delta_{T,0}^{(S)}(q,t) - \frac{1}{2}\omega_c P_2(\mu)\Pi(q,t)$$
$$+\frac{4iq\mu}{a(t)}\omega_c(t)\delta u_{B\,q}(t) - 2\dot{A}_q(t) + 2q^2\mu^2\dot{B}_q(t)$$

$$\dot{\Delta}_P^{(S)}(q,\mu,t) + i\frac{q\mu}{a(t)}\Delta_P^{(S)}(q,\mu,t) = -\omega_c(t)\Delta_P^{(S)}(q,\mu,t)$$
$$+\frac{3}{4}\omega_c(t)(1-\mu^2)\Pi(q,t)$$

with source function

$$\Pi = \Delta_{P,0}^{(S)} + \Delta_{T,2}^{(S)} + \Delta_{P,2}^{(S)}$$

Line-of-sight integration

A formal solution is obtained by line-of-sight integration

$$\Delta_T^{(S)}(q,\mu,t_0) = \int_{t_1}^{t_0} dt\ \exp\left[-iq\mu\int_t^{t_0}\frac{dt'}{a(t')} - \int_t^{t_0} dt'\omega_c(t')\right]$$

$$\times\left\{\omega_c\left[\Delta_{T,0}^{(S)} - \frac{1}{2}P_2(\mu)\Pi(q,t) - 2a^2(t)\ddot{B}_q(t) - 2a(t)\dot{a}(t)\dot{B}_q(t)\right.\right.$$

$$\left. + 4i\mu q\left(\delta u_q(t)/a(t) + a(t)\dot{B}_q(t)/2\right)\right]$$

$$\left. - \frac{d}{dt}\left(2A_q(t) + 2a^2(t)\ddot{B}_q(t) + 2a(t)\dot{a}(t)\dot{B}_q(t)\right)\right\}$$

Only depends on the first few multipoles and can be used to speed up the computation significantly by truncating the hierarchy and using this solution.

Initial Conditions

What remains is the choice of initial conditions

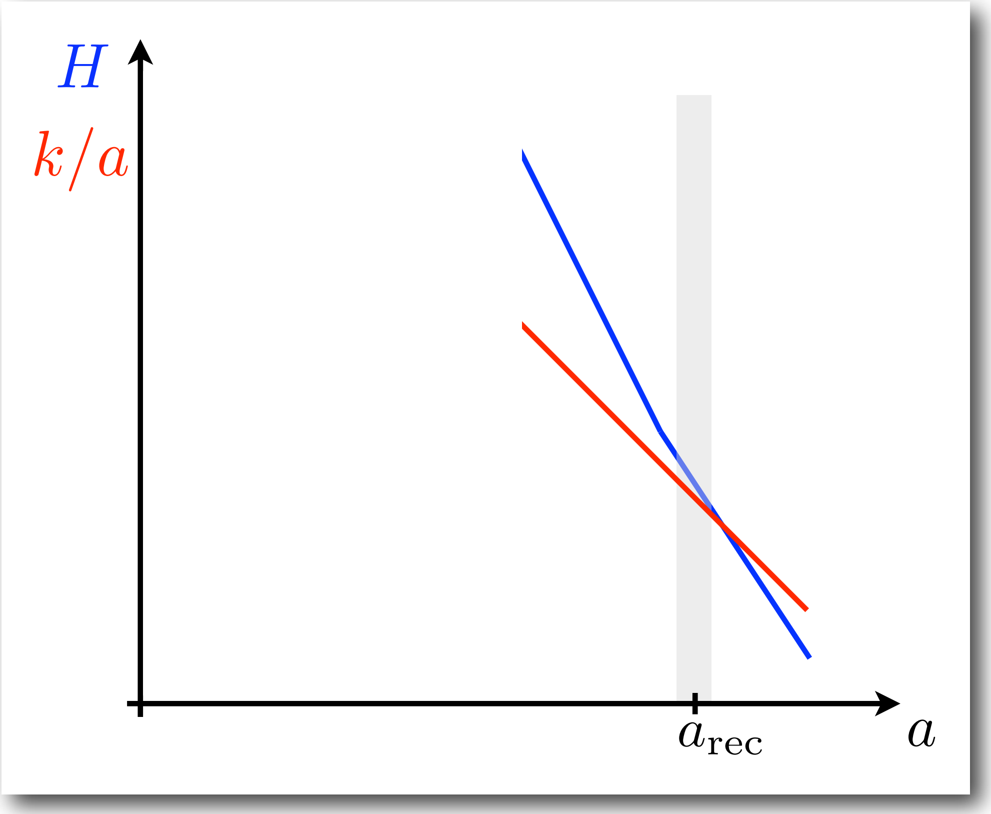

All modes are "outside the horizon" at early times.

$$\frac{q}{a} \ll H$$

Initial Conditions

At early times the Boltzmann hierarchy for photons reduces to the equations of hydrodynamics and we can look for solutions of the form

$$\Delta_{T,0}^{(S)} = \Delta_{\nu,0}^{(S)} = \frac{4}{3}\frac{\delta\rho_c}{\bar{\rho}_c} = \frac{4}{3}\frac{\delta\rho_b}{\bar{\rho}_b} \equiv \Delta_0^{(S)}$$

$$\Delta_{\nu,1}^{(S)} \propto \Delta_{T,1}^{(S)} = -\frac{4}{3}\frac{q}{a}\delta u_{b\,q} \equiv \Delta_1^{(S)}$$

$$\Delta_{T,\ell} \to 0 \quad \text{for} \quad \ell \geq 2$$

$$\Delta_{P,\ell} \to 0$$

These are adiabatic initial conditions

Initial Conditions

In this limit $\mathcal{R}_q = \frac{A_q}{2} + H\delta u_q$ becomes a constant

and we can normalize our solution such that $\mathcal{R}_q \to \mathcal{R}_q^o$

Then

$$\Delta_0^{(S)}(q,t) = \frac{4}{3}\frac{q^2t^2}{a^2(t)}\mathcal{R}_q^o\,,$$

$$\Delta_1^{(S)}(q,t) = \frac{8}{27}\frac{q^3t^3}{a^3(t)}\mathcal{R}_q^o\,,$$

$$\Delta_{\nu,2}^{(S)}(q,t) = -\frac{16}{3(15+4f_\nu)}\frac{q^2t^2}{a^2(t)}\mathcal{R}_q^o\,,$$

$$A_q(t) = \left(2 - \frac{2}{3}\frac{5+4f_\nu}{15+4f_\nu}\frac{q^2t^2}{a^2(t)}\right)\mathcal{R}_q^o\,,$$

$$q^2\dot{B}_q(t) = \frac{20}{15+4f_\nu}\frac{q^2t}{a^2(t)}\mathcal{R}_q^o\,,$$

$$\Delta_{\nu,1}^{(S)}(q,t) = \frac{23+4f_\nu}{15+4f_\nu}\Delta_1^{(S)}(q,t)$$

Initial Conditions

Boltzmann codes such as CAMB or CLASS solve these equations given adiabatic initial conditions.

With the solution at hand, one computes

$$a^{(S)}_{T,\ell m} = \pi T_0 i^\ell \int d^3q \; \alpha(\mathbf{q}) Y_\ell^{m*}(\hat{q}) \Delta^{(S)}_{T,\ell}(q,t_0)$$

or directly

$$C^{(S)}_{TT,\ell} = \pi^2 T_0^2 \int q^2 dq \; \left|\Delta^{(S)}_{T,\ell}(q,t_0)\right|^2$$

similarly for polarization and tensor contribution

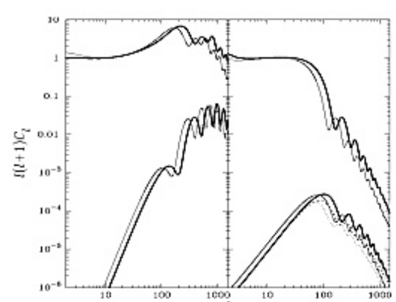

Code for Anisotropies in the Microwave Background

by Antony Lewis and Anthony Challinor

CLASS

the Cosmic Linear Anisotropy Solving System

Julien Lesgourgues

More on temperature anisotropies

From the line-of-sight solution

$$\Delta_T^{(S)}(q,\mu,t_0) = \int_{t_1}^{t_0} dt\ \exp\left[-iq\mu\int_t^{t_0}\frac{dt'}{a(t')} - \int_t^{t_0} dt'\omega_c(t')\right]$$
$$\times\left\{\omega_c\left[\Delta_{T,0}^{(S)} - \frac{1}{2}P_2(\mu)\Pi(q,t) - 2a^2(t)\ddot{B}_q(t) - 2a(t)\dot{a}(t)\dot{B}_q(t)\right.\right.$$
$$\left. +4i\mu q\left(\delta u_q(t)/a(t) + a(t)\dot{B}_q(t)/2\right)\right]$$
$$\left. - \frac{d}{dt}\left(2A_q(t) + 2a^2(t)\ddot{B}_q(t) + 2a(t)\dot{a}(t)\dot{B}_q(t)\right)\right\}$$

we see that the temperature perturbations consist of two contributions

$$\left(\frac{\Delta T(\hat{n})}{T_0}\right)^{(S)} = \left(\frac{\Delta T(\hat{n})}{T_0}\right)^{(S)}_{LSS} + \left(\frac{\Delta T(\hat{n})}{T_0}\right)^{(S)}_{ISW}$$

More on temperature anisotropies

$$\left(\frac{\Delta T(\hat{n})}{T_0}\right)^{(S)}_{LSS} = \int \frac{d^3q}{(2\pi)^3}\alpha(\vec{q})$$

$$\times \int\limits_{t_1}^{t_0} dt \ \exp\left[-iq\mu \int_t^{t_0} \frac{dt'}{a(t')}\right] \exp\left[-\int_t^{t_0} dt'\omega_c(t')\right] \omega_c(t)$$

$$\times \left[\frac{1}{4}\Delta^{(S)}_{T,0}(q,t) - \frac{1}{8}P_2(\mu)\Pi(q,t) - \frac{1}{2}a^2(t)\ddot{B}_q(t) - \frac{1}{2}a(t)\dot{a}(t)\dot{B}_q(t)\right.$$

$$\left. + i\mu q\left(\delta u_q(t)/a(t) + a(t)\dot{B}_q(t)/2\right)\right]$$

More on temperature anisotropies

$$\left(\frac{\Delta T(\hat{n})}{T_0}\right)^{(S)}_{LSS} = \int \frac{d^3q}{(2\pi)^3}\alpha(\vec{q})$$

Last scattering probability

$$\times \int_{t_1}^{t_0} dt \ \exp\left[-iq\mu\int_t^{t_0}\frac{dt'}{a(t')}\right]\exp\left[-\int_t^{t_0} dt'\omega_c(t')\right]\omega_c(t)$$

$$\times\left[\frac{1}{4}\Delta^{(S)}_{T,0}(q,t) - \frac{1}{8}P_2(\mu)\Pi(q,t) - \frac{1}{2}a^2(t)\ddot{B}_q(t) - \frac{1}{2}a(t)\dot{a}(t)\dot{B}_q(t)\right.$$

$$\left. + i\mu q\left(\delta u_q(t)/a(t) + a(t)\dot{B}_q(t)/2\right)\right]$$

More on temperature anisotropies

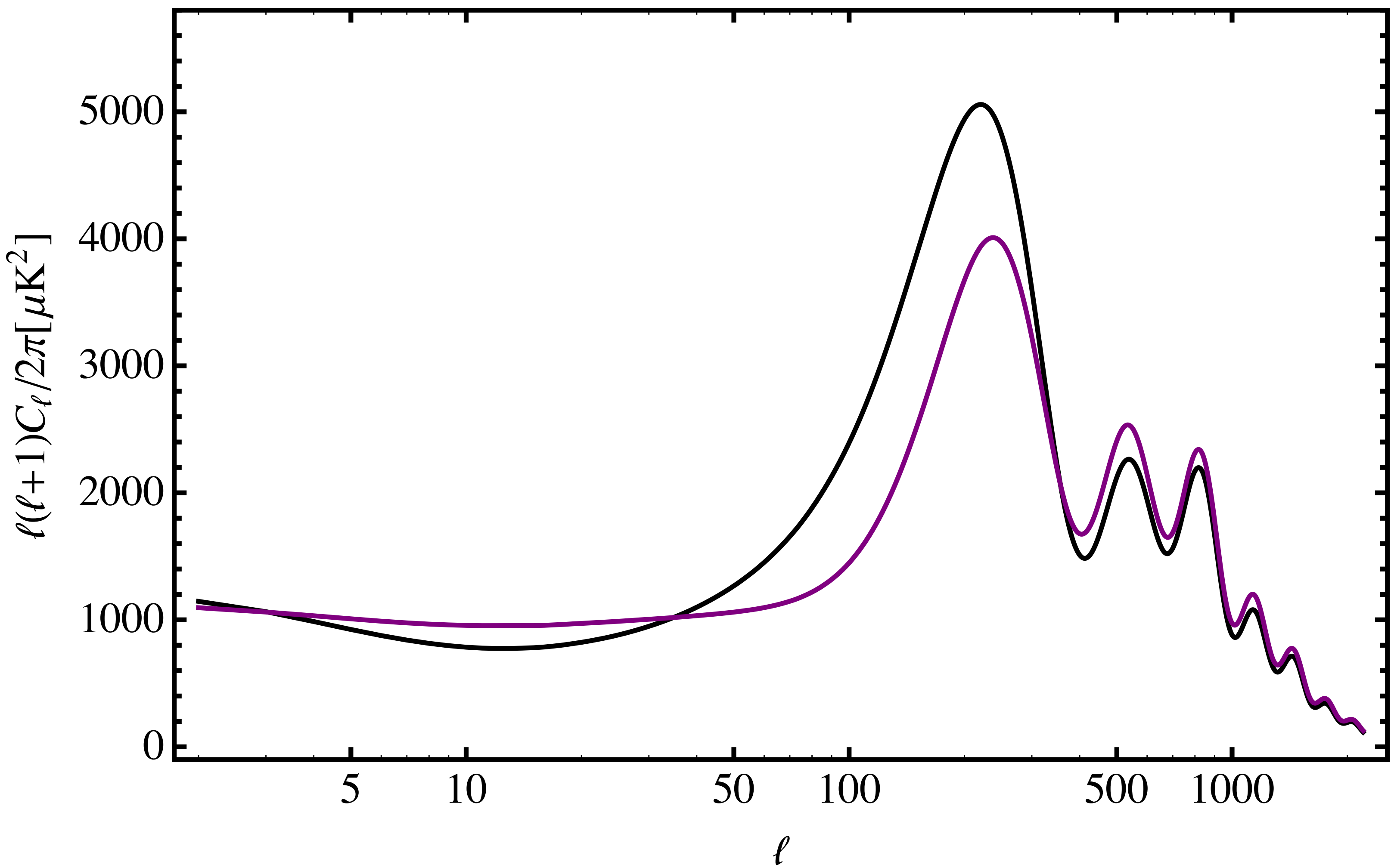

More on temperature anisotropies

$$\left(\frac{\Delta T(\hat{n})}{T_0}\right)^{(S)}_{LSS} = \int \frac{d^3q}{(2\pi)^3}\alpha(\vec{q})$$

$$\times \int_{t_1}^{t_0} dt\ \exp\left[-iq\mu\int_t^{t_0}\frac{dt'}{a(t')}\right]\exp\left[-\int_t^{t_0} dt'\omega_c(t')\right]\omega_c(t)$$

$$\times\left[\frac{1}{4}\Delta^{(S)}_{T,0}(q,t) - \frac{1}{8}P_2(\mu)\Pi(q,t) - \frac{1}{2}a^2(t)\ddot{B}_q(t) - \frac{1}{2}a(t)\dot{a}(t)\dot{B}_q(t)\right.$$

$$\left. + i\mu q\left(\delta u_q(t)/a(t) + a(t)\dot{B}_q(t)/2\right)\right]$$

Intrinsic density fluctuation and gravitational redshifting

More on temperature anisotropies

$$\left(\frac{\Delta T(\hat{n})}{T_0}\right)^{(S)}_{LSS} = \int \frac{d^3q}{(2\pi)^3}\alpha(\vec{q})$$

$$\times \int_{t_1}^{t_0} dt \ \exp\left[-iq\mu \int_t^{t_0} \frac{dt'}{a(t')}\right] \exp\left[-\int_t^{t_0} dt' \omega_c(t')\right] \omega_c(t)$$

$$\times \left[\frac{1}{4}\Delta^{(S)}_{T,0}(q,t) - \frac{1}{8}P_2(\mu)\Pi(q,t) - \frac{1}{2}a^2(t)\ddot{B}_q(t) - \frac{1}{2}a(t)\dot{a}(t)\dot{B}_q(t)\right.$$

$$\left. + i\mu q\left(\delta u_q(t)/a(t) + a(t)\dot{B}_q(t)/2\right)\right]$$

Intrinsic density fluctuation and gravitational redshifting

Doppler effect

More on temperature anisotropies

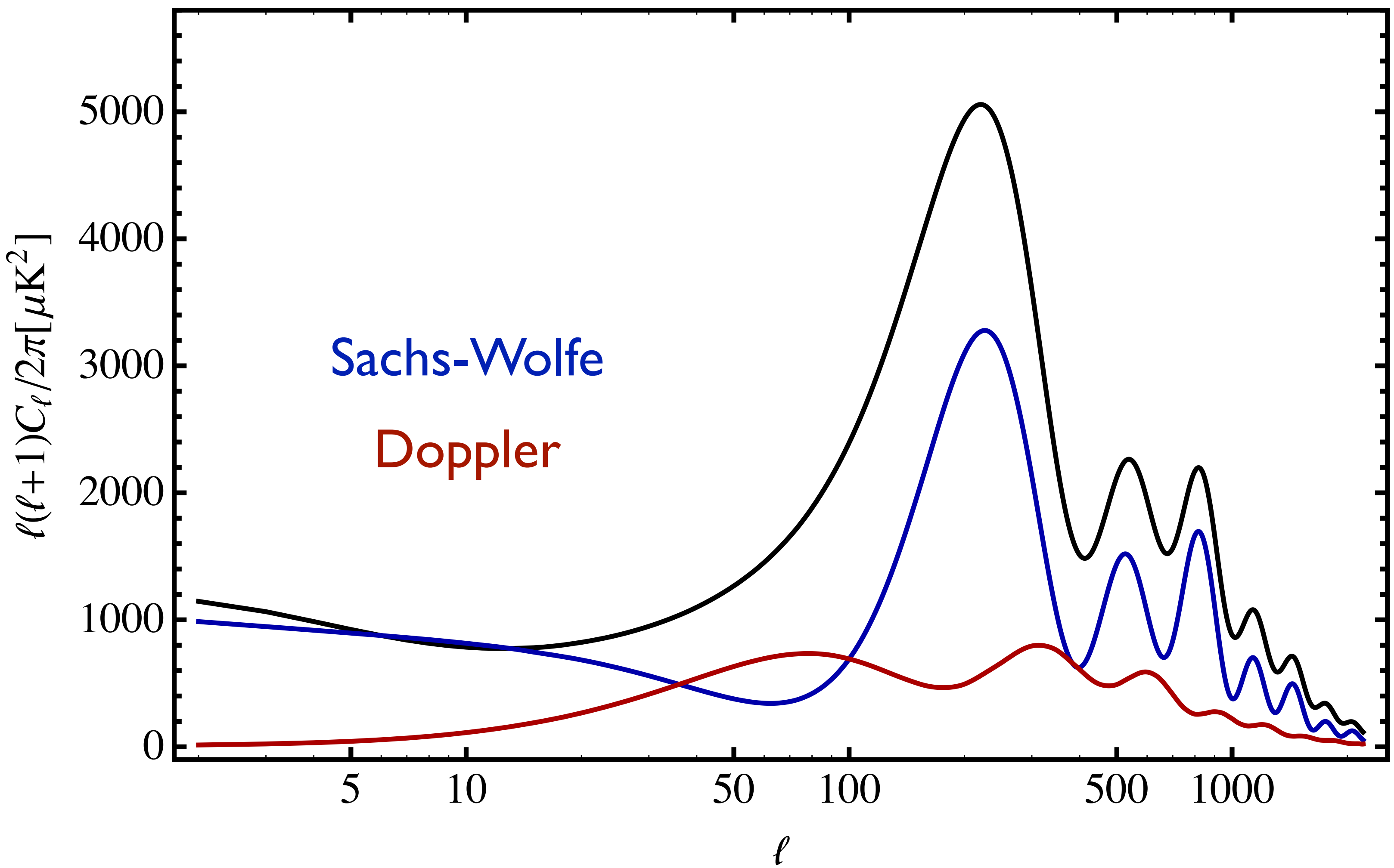

More on temperature anisotropies

Integrated Sachs-Wolfe effect

$$\left(\frac{\Delta T(\hat{n})}{T_0}\right)^{(S)}_{ISW} = -\frac{1}{2}\int \frac{d^3q}{(2\pi)^3}\alpha(\vec{q})$$

$$\times \int_{t_1}^{t_0} dt\ \exp\left[-iq\mu\int_t^{t_0}\frac{dt'}{a(t')}\right]\exp\left[-\int_t^{t_0} dt'\omega_c(t')\right]$$

$$\times\frac{d}{dt}\Big(A_q(t) + a^2(t)\ddot{B}_q(t) + a(t)\dot{a}(t)\dot{B}_q(t)\Big)$$

This contribution can be generated even in the absence of free electrons.

More on temperature anisotropies

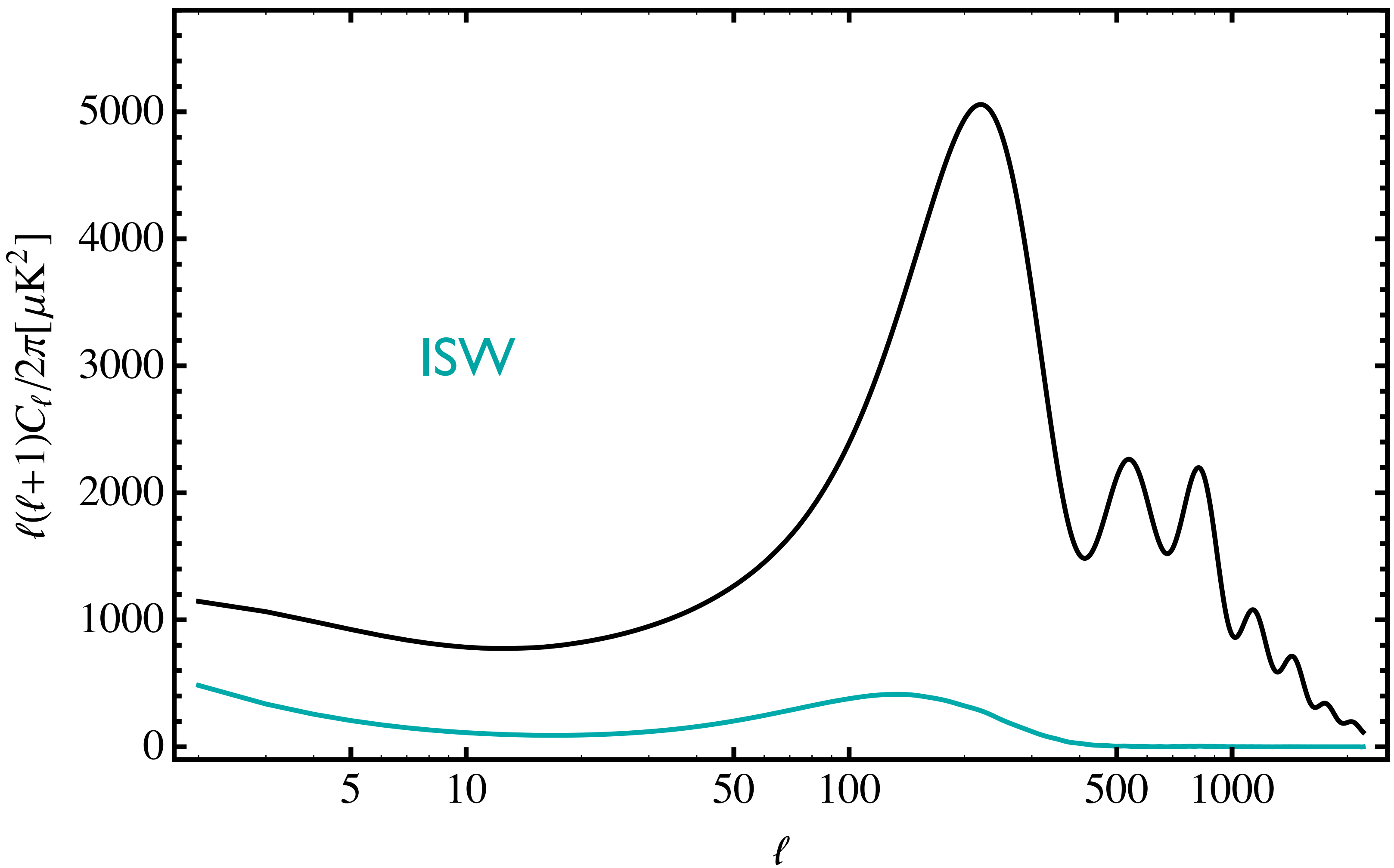

More on temperature anisotropies

During matter domination the gravitational potential does not evolve

$$\frac{d}{dt}\left(A_q(t) + a^2(t)\ddot{B}_q(t) + a(t)\dot{a}(t)\dot{B}_q(t)\right) = 0$$

The integrated Sachs-Wolfe effect has two contributions

early contribution:

During recombination radiation is not yet completely negligible.

late contribution:

At late times dark energy becomes important

More on temperature anisotropies

Early vs late ISW

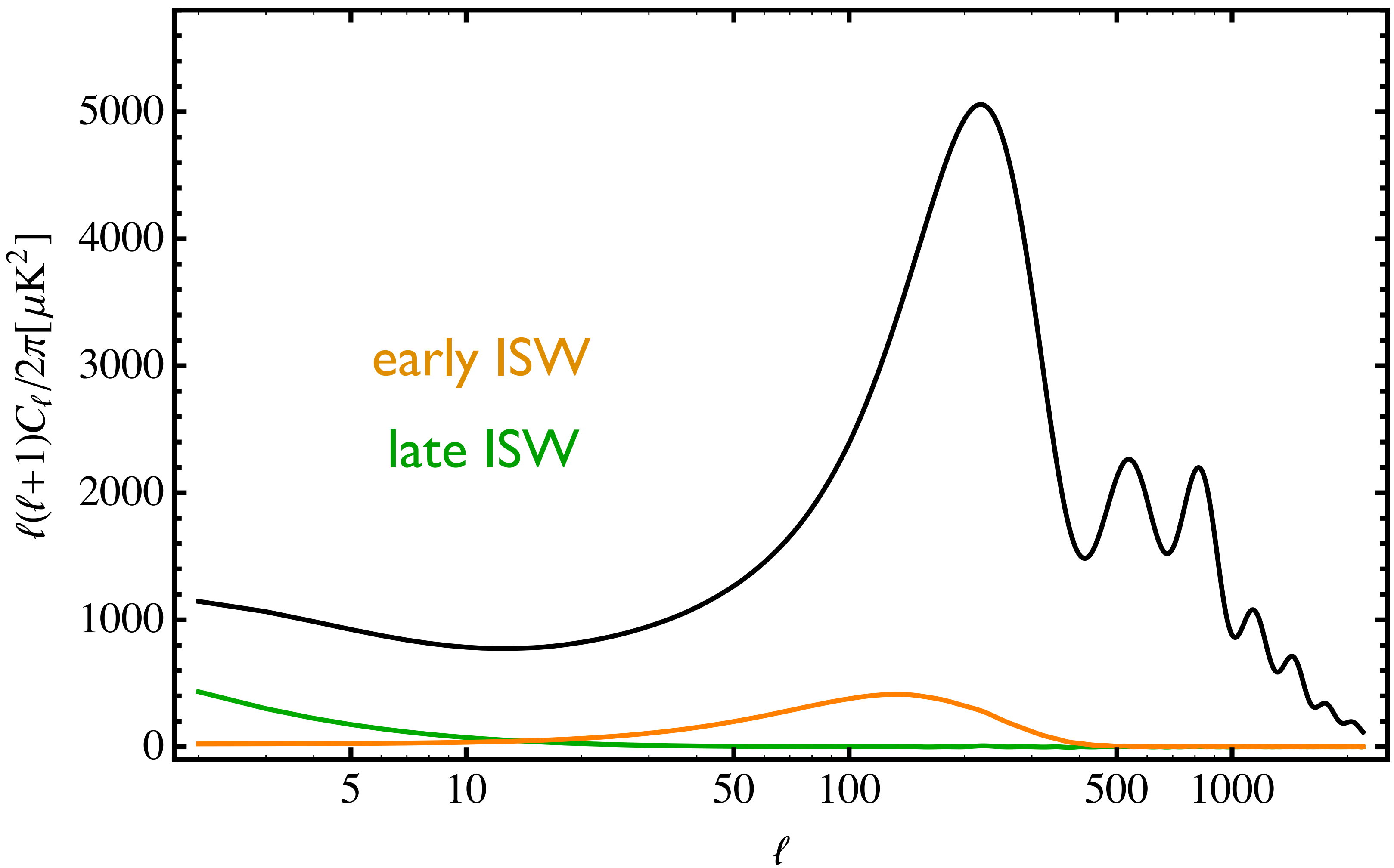

More on temperature anisotropies

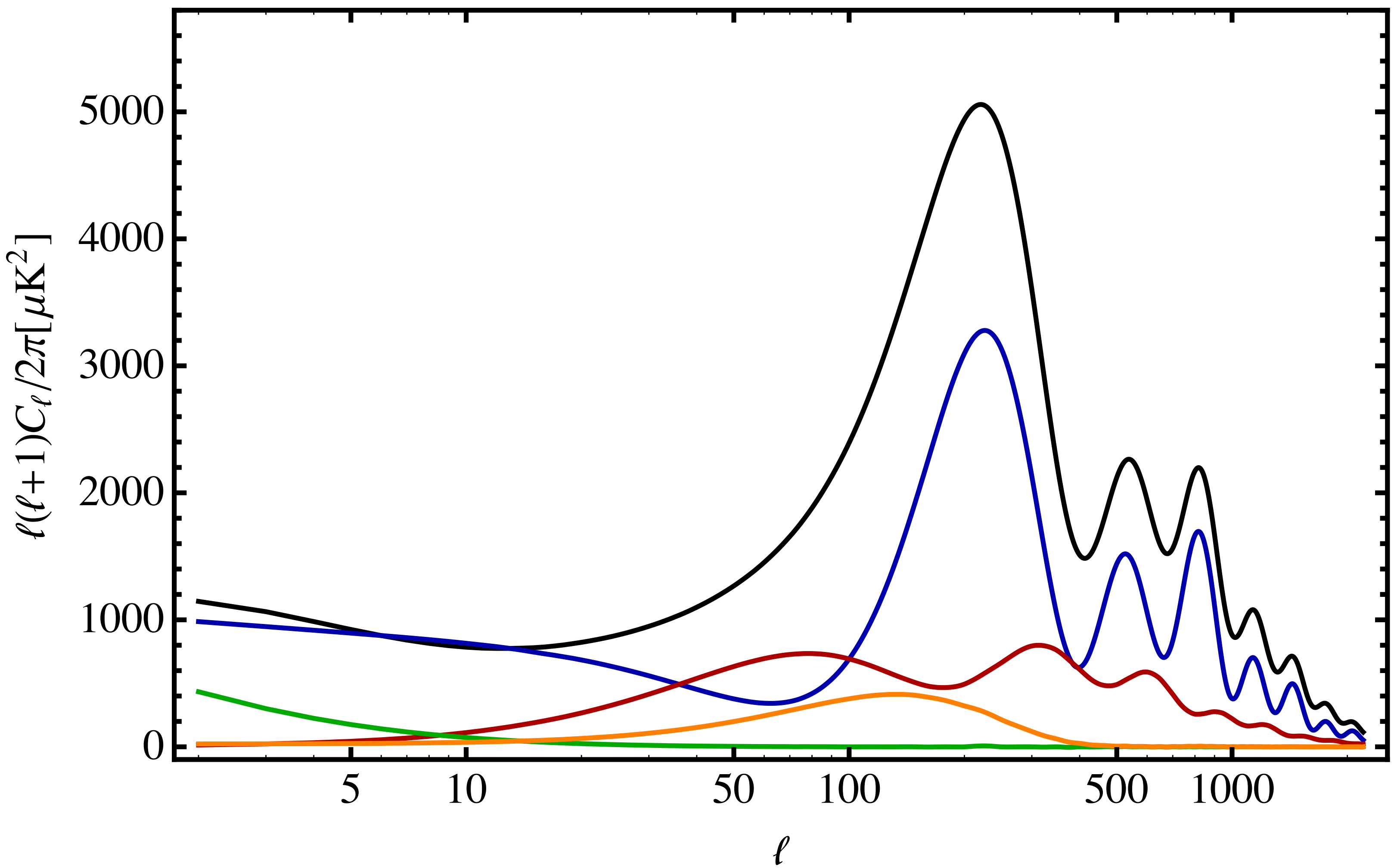

More on temperature anisotropies

Recombination vs late time contributions

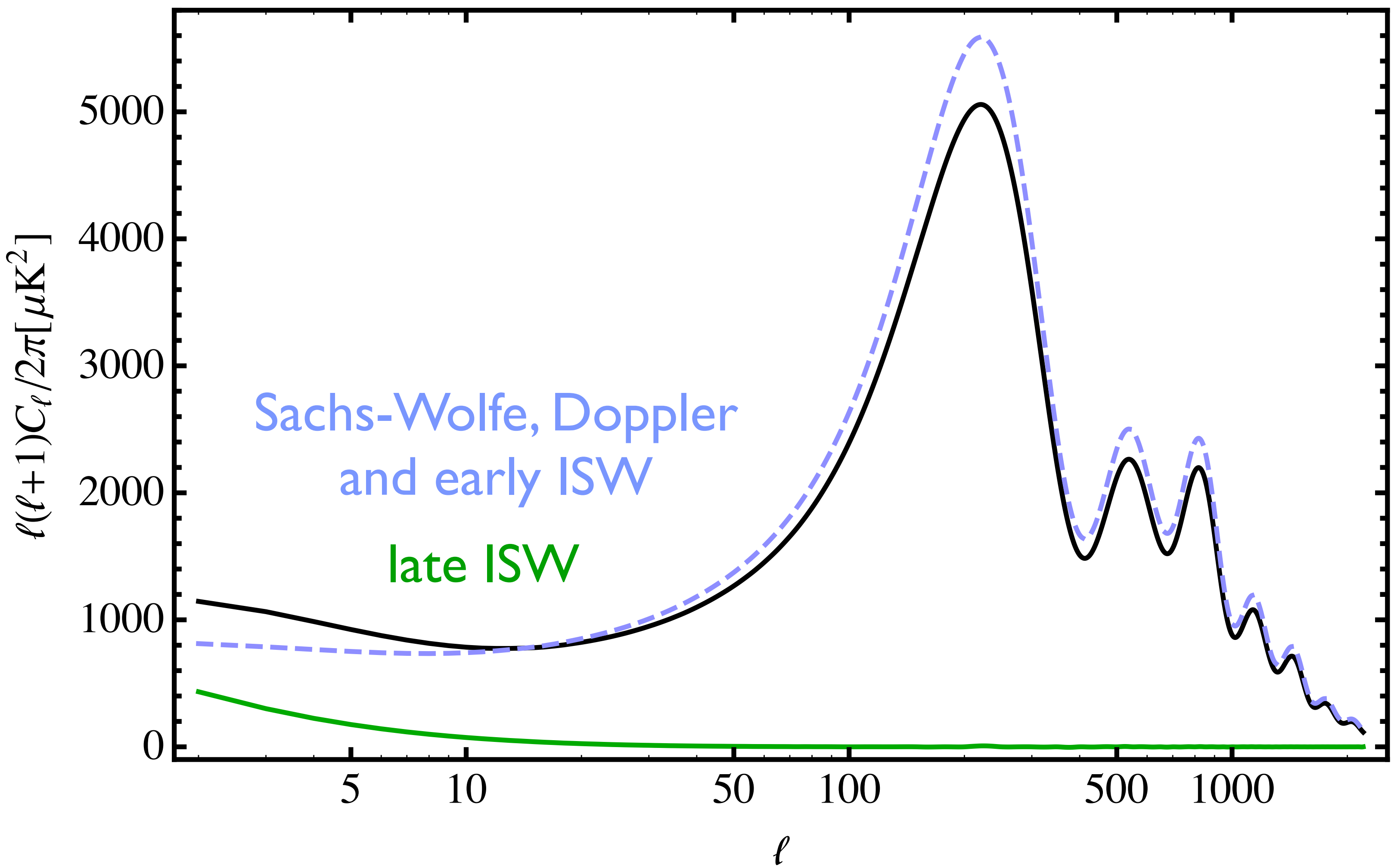

More on temperature anisotropies

Recombination vs late time contributions

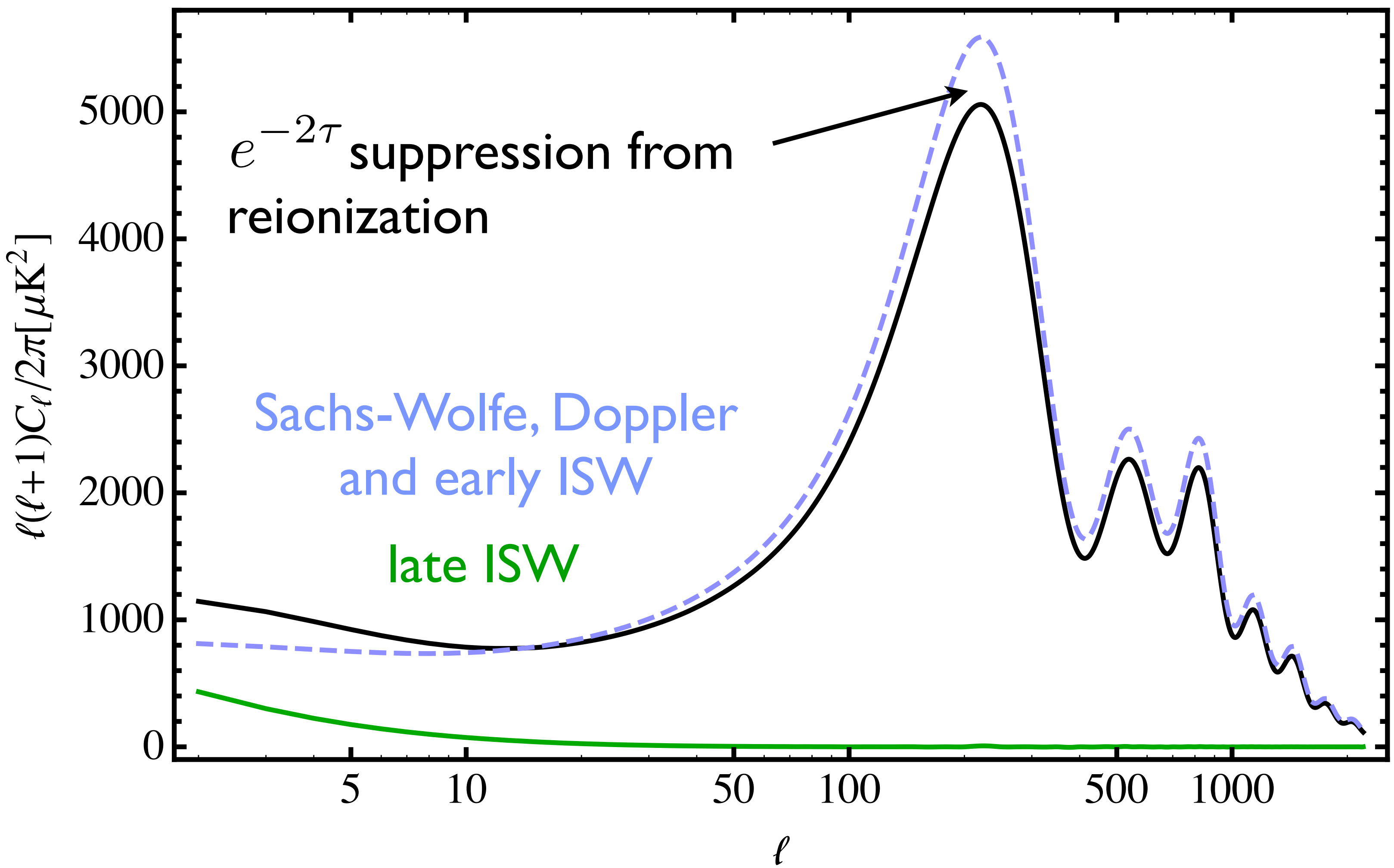

Beyond Primary Anisotropies

CMB data consists of sky maps at different microwave frequencies

COBE (DMR)
(1989-93)

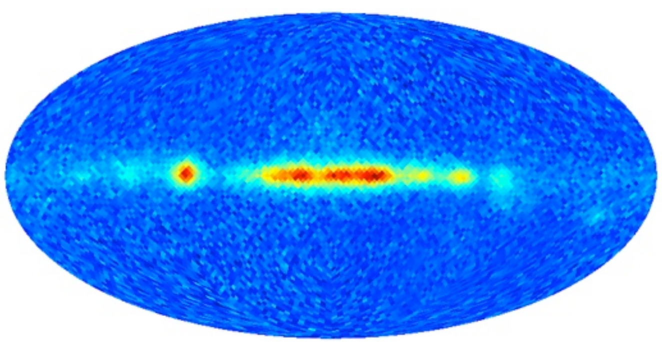

31 GHz

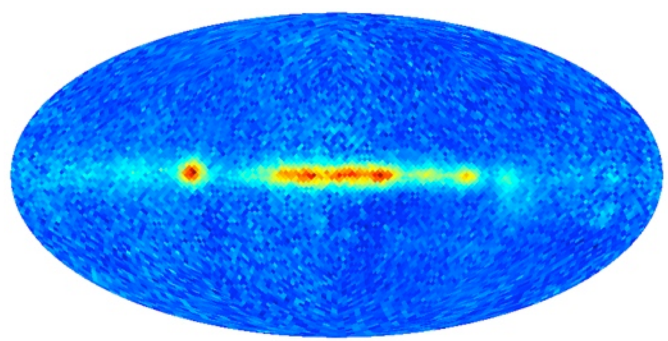

53 GHz

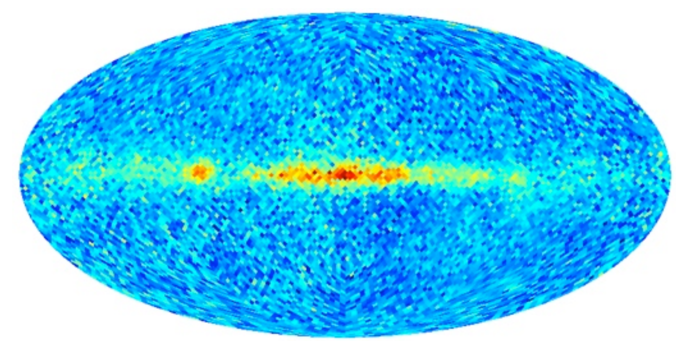

91 GHz

Beyond Primary Anisotropies

WMAP
(2001-10)

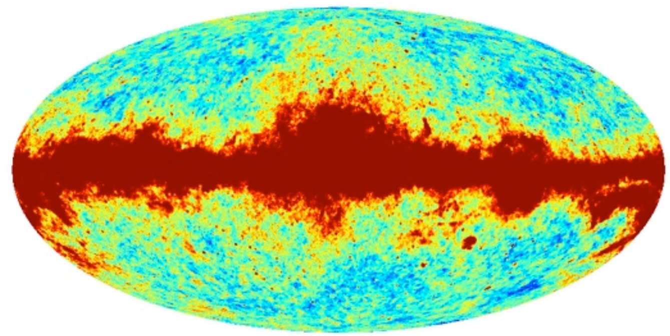

23 GHz

33 GHz

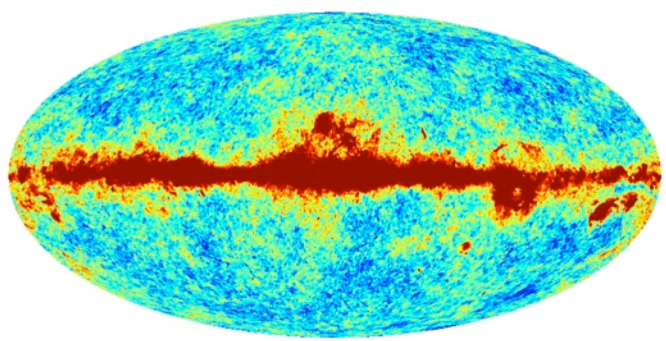

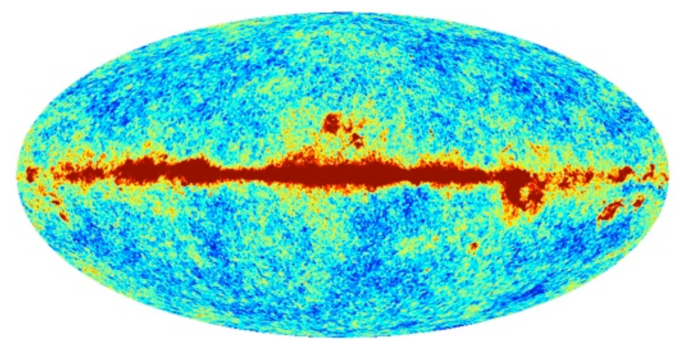

41 GHz

61 GHz

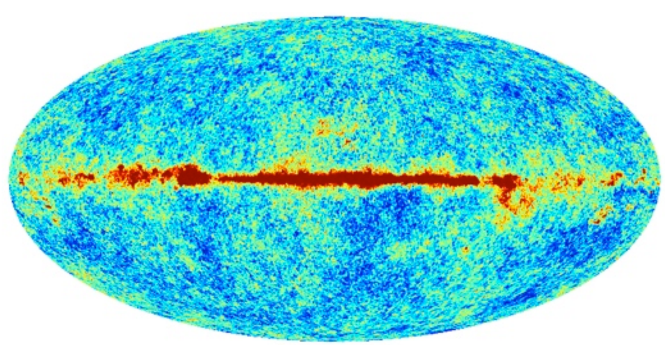

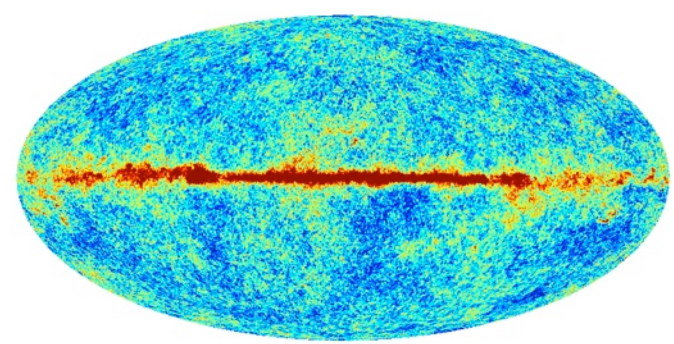

94 GHz

Beyond Primary Anisotropies

Planck (2009-15)

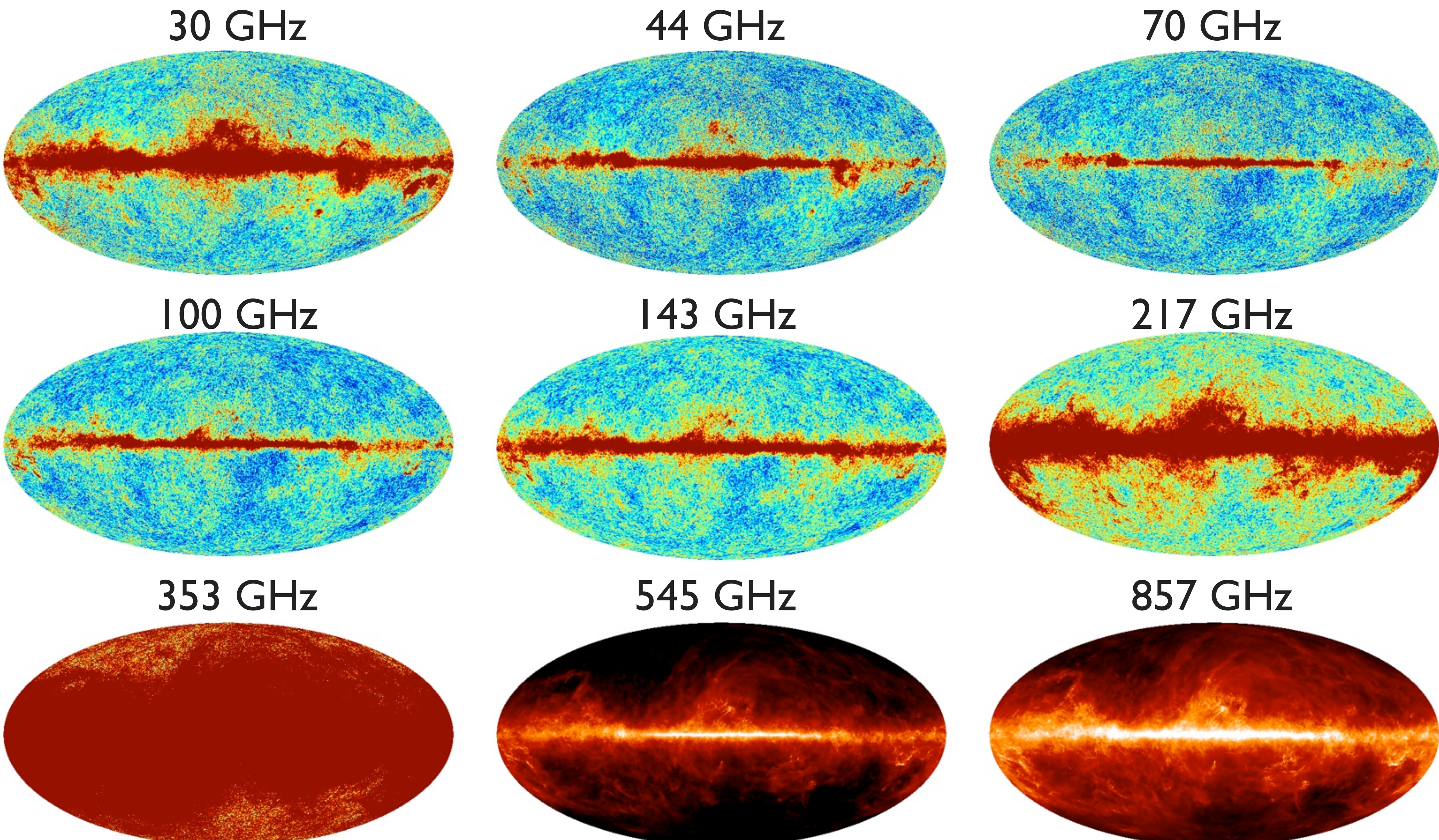

Beyond Primary Anisotropies

To learn about the CMB this means we must understand

- Galactic dust
- Galactic synchrotron
- CO
- CIB
- dusty point sources
- radio point sources
- zodiacal light
- ...

Beyond Primary Anisotropies

We have additional ways to probe cosmology

- Reionization
- Thermal SZ effect
- Kinetic SZ effect
- Lensing of the CMB
- ...

Thermal SZ effect

The change in temperature is set by

$$\Delta T(\hat{n}) = y(\hat{n})\,(x\coth(x/2) - 4)\,T_0$$

$$x = \frac{h\nu}{kT} \qquad\qquad y(\hat{n}) = \int dl\, n_e \sigma_T \frac{kT_e}{m_e}$$

A map of the Compton parameter y is a measure of hot gas in the universe between us and the surface of last scattering.

Thermal SZ effect

SZ view of Abell 2319 with Planck

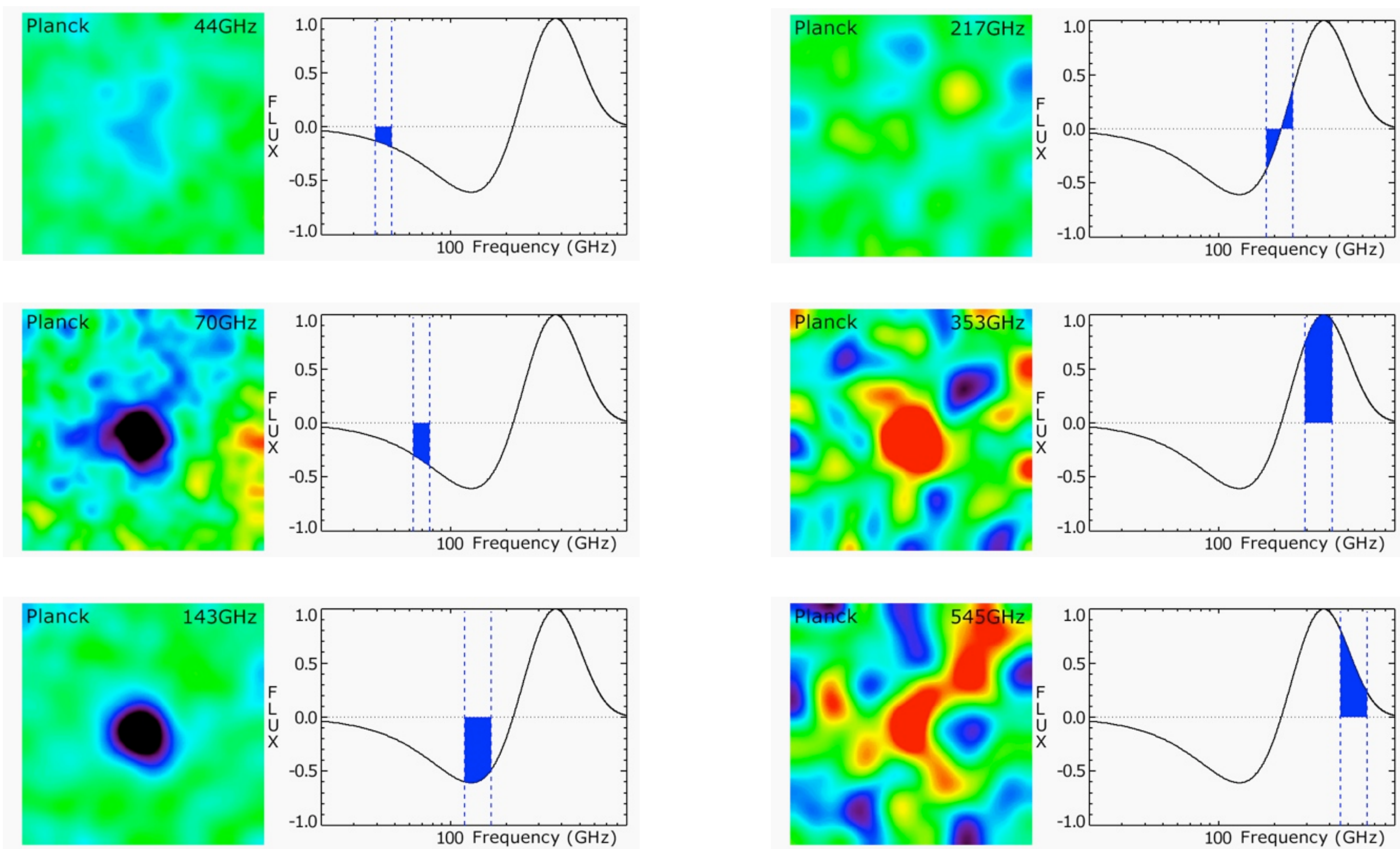

Thermal SZ effect

Planck SZ clusters

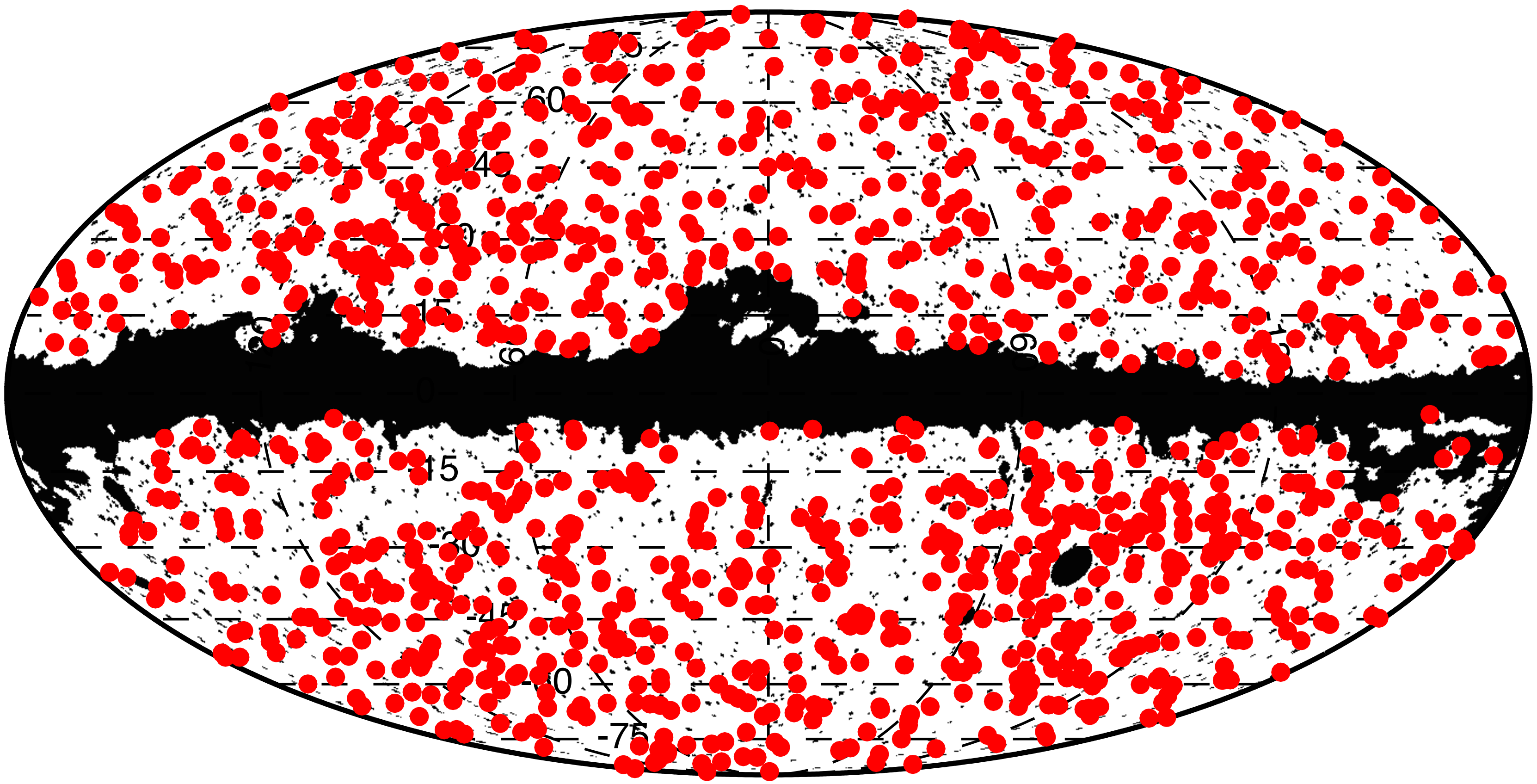

Thermal SZ effect

Planck thermal SZ power spectrum

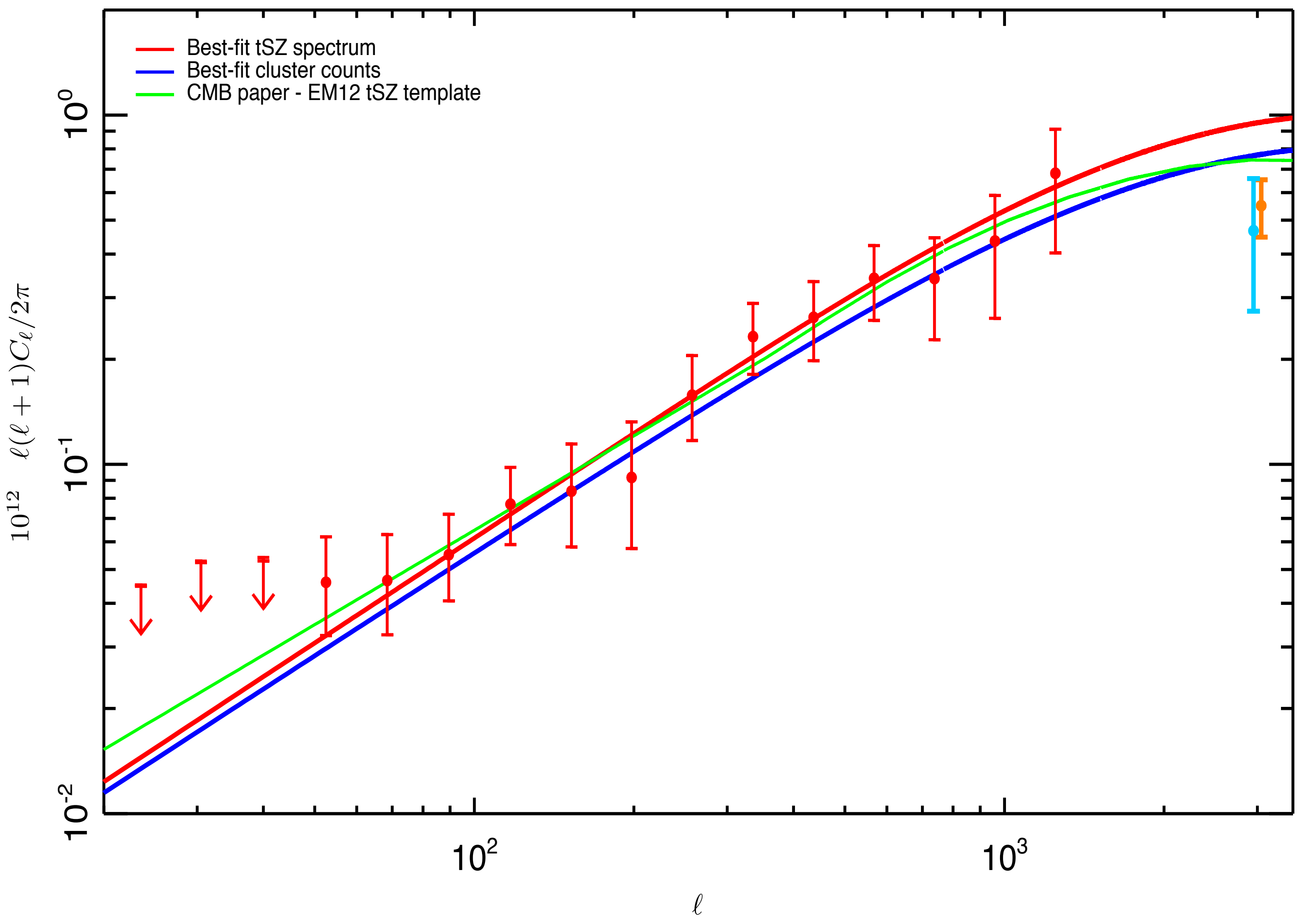

Thermal SZ effect

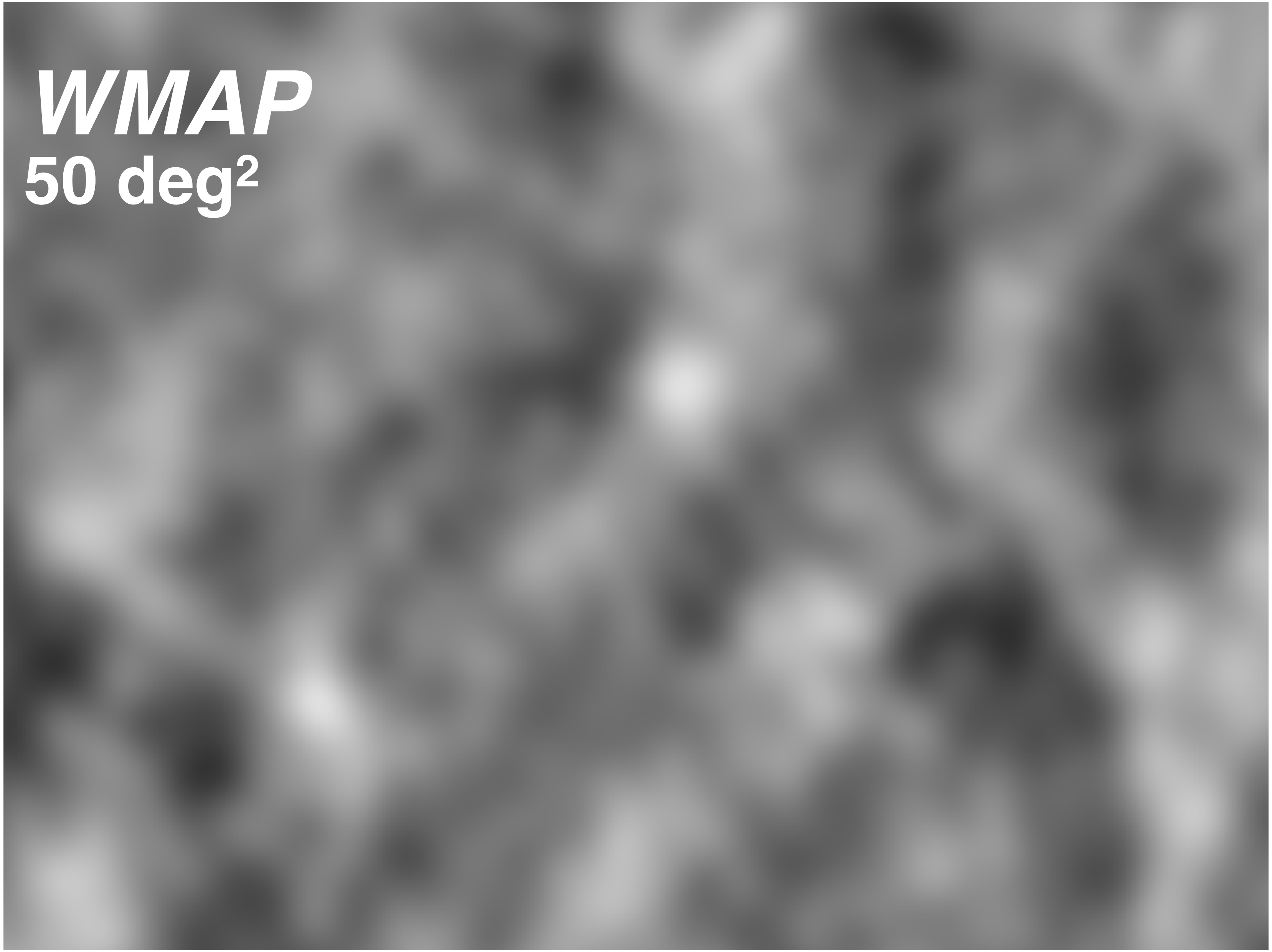

Thermal SZ effect

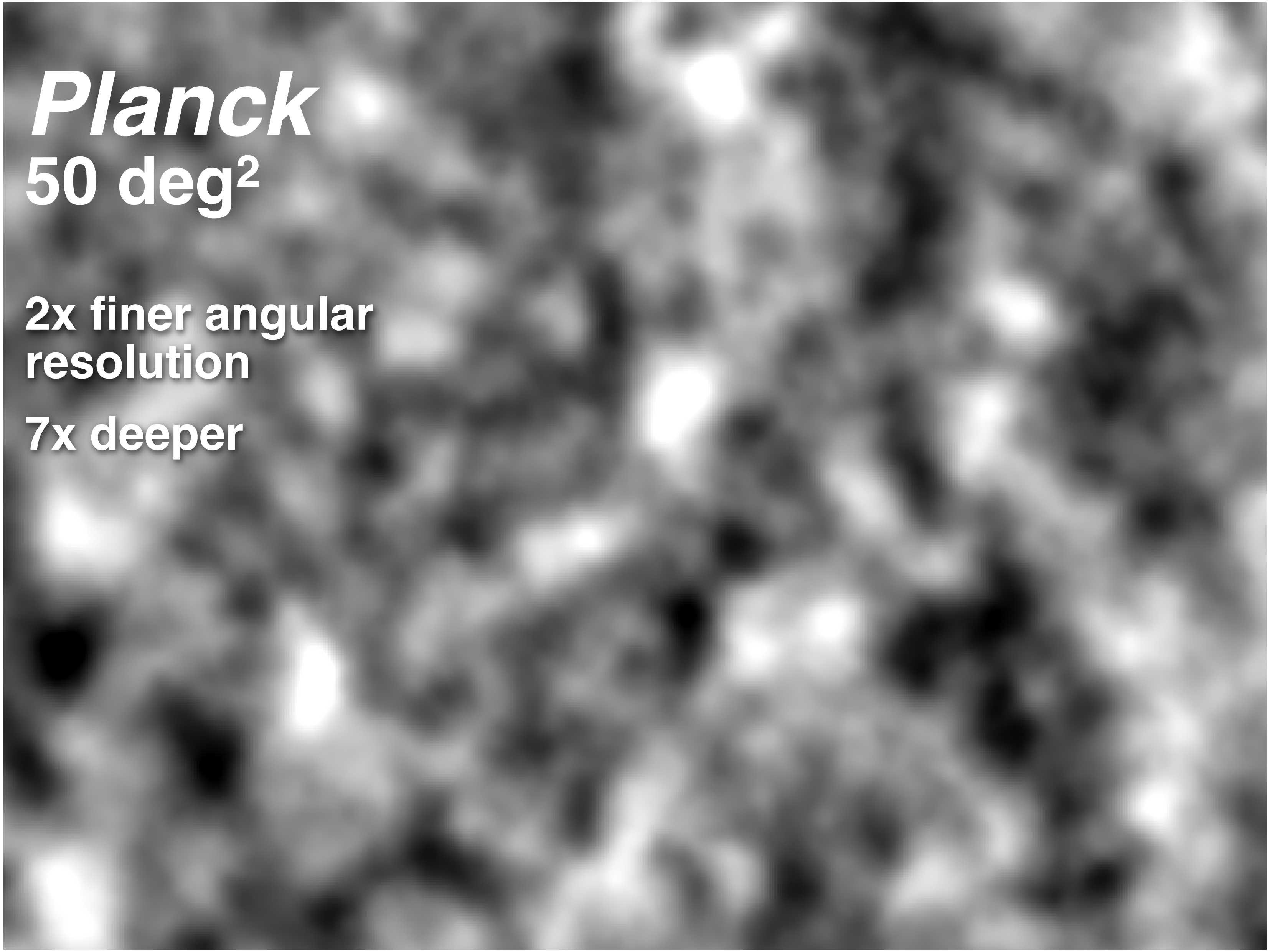

Thermal SZ effect

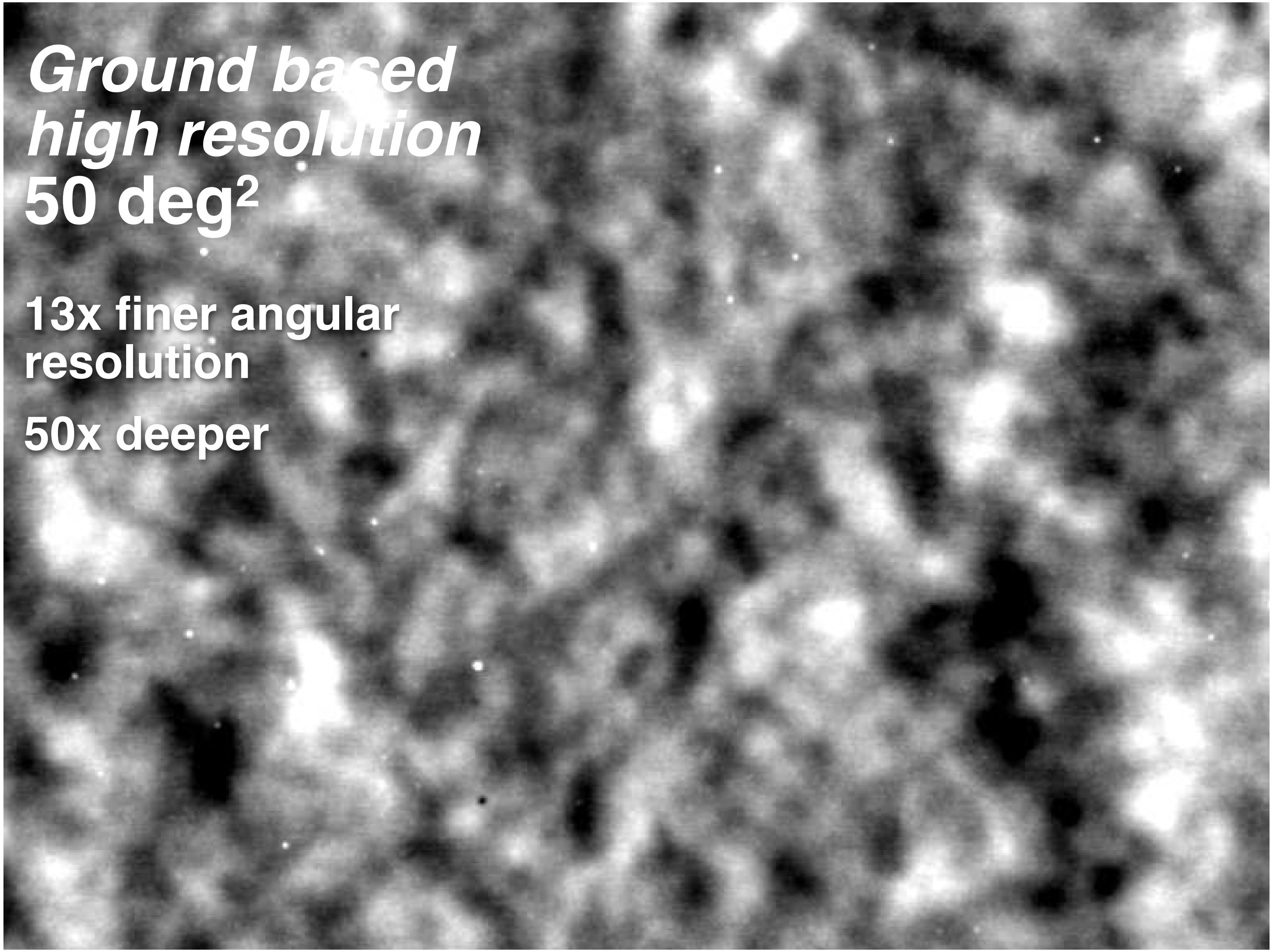

Lensing

$$T(\hat{n}) = T^{\mathrm{unlensed}}\left(\hat{n} + \nabla\phi(\hat{n})\right)$$

- Washes out acoustic peaks in the power spectrum (this effect is included in all the analyses)
- leads to temperature three-point correlations because of correlations between ISW and lensing
- leads to temperature four-point correlations proportional to power spectrum of lensing field

$$\mathbb{T}^{\ell_1\ell_2}_{\ell_3\ell_4}(L) \approx C_L^{\phi\phi} C_{\ell_2}^{TT} C_{\ell_4}^{TT} F_{\ell_1 L \ell_2} F_{\ell_3 L \ell_4}$$

Lensing

Detected at high significance (40σ)

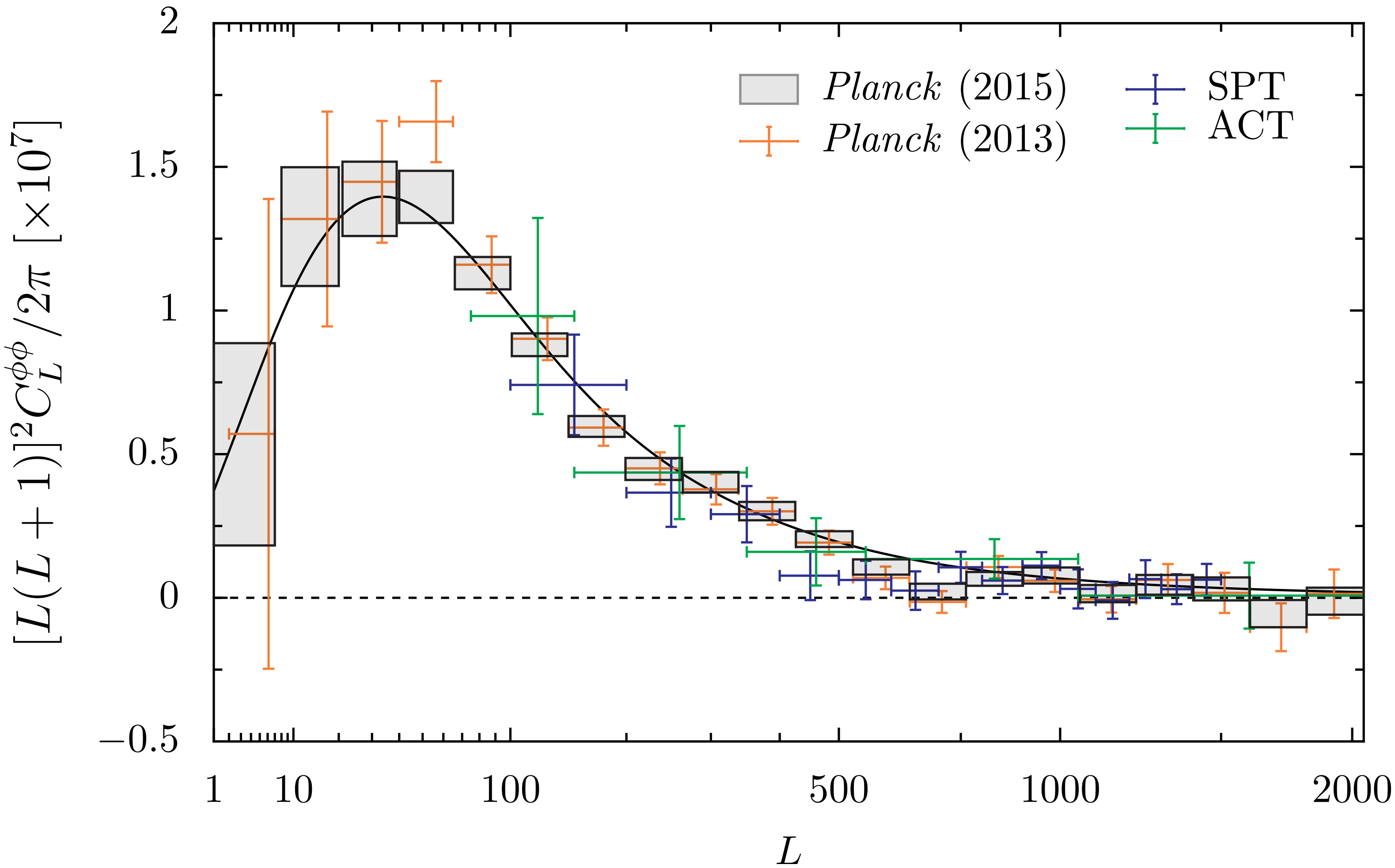

Lensing

The lensing potential itself can also be reconstructed

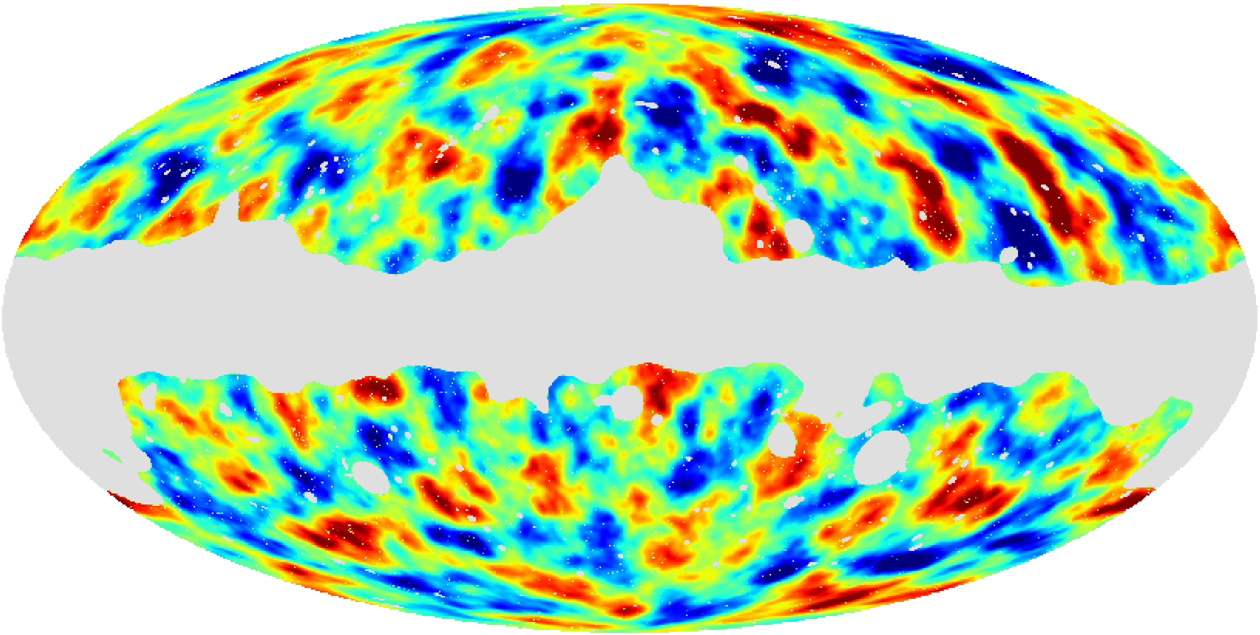

and provides a map (albeit a noisy one) of (the projection of) all matter between us and the surface of last scattering!

Ideal measurement

ΔT $\qquad$ Q $\qquad$ U

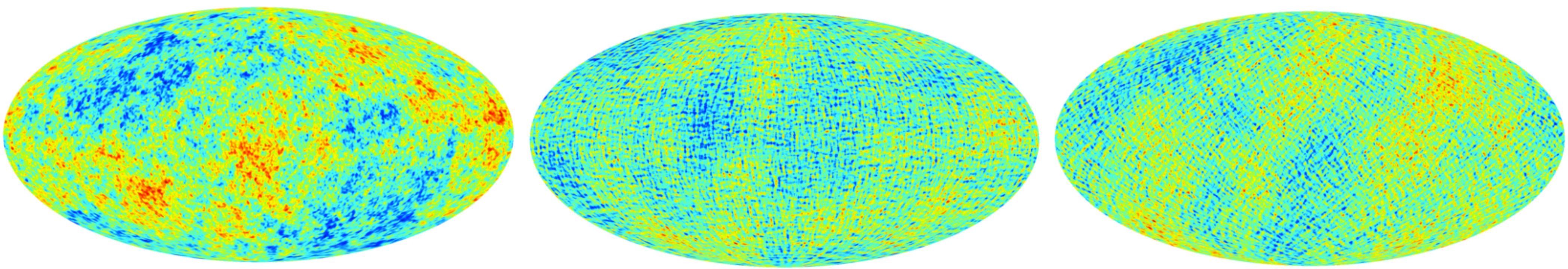

$$a_{T,\ell m} = \int d^2\hat{n}\, Y_\ell^{m*}(\hat{n}) \Delta T(\hat{n})$$

$$a_{E,\ell\, m}, a_{B,\ell\, m}$$

$$C_{TT,\ell}^{\mathrm{obs}} \equiv \frac{1}{2\ell+1} \sum_m \left| a_{T,\ell\, m}^{\mathrm{obs}} \right|^2$$

$$C_{TE,\ell}^{\mathrm{obs}}, C_{EE,\ell}^{\mathrm{obs}}, C_{BB,\ell}^{\mathrm{obs}}$$

Ideal measurement

http://healpix.sourceforge.net/

or in Python https://healpy.readthedocs.io/en/latest/

Ideal measurement

How do we estimate the cosmological parameters of our favorite model?

Denote the parameters by $\vec{\theta}$ and the data by D where D could be $a_{\ell m}^{\mathrm{obs}}, C_\ell^{\mathrm{obs}}$

We would like to know $P(\vec{\theta}|D)$

We cannot compute it directly, but can use Bayes' theorem

$$P(\vec{\theta}|D) = \frac{P(D|\vec{\theta})P(\vec{\theta})}{P(D)}$$

"prior"

Ideal measurement

How do we estimate the cosmological parameters of our favorite model?

Denote the parameters by $\vec{\theta}$ and the data by D
where D could be $a_{\ell m}^{\rm obs}, C_\ell^{\rm obs}$

We would like to know $P(\vec{\theta}|D)$

We cannot compute it directly, but can use Bayes' theorem

$$P(\vec{\theta}|D) = \frac{P(D|\vec{\theta})P(\vec{\theta})}{P(D)}$$

"prior"

This suggests to define a likelihood for our experiment

$$\mathcal{L}(\vec{\theta}) = P(D|\vec{\theta})$$

which can be computed for any given theory

Ideal measurement

Warm up: Measurement of temperature anisotropies

For Gaussian perturbations

$$\langle a_{\ell\, m} a^*_{\ell'\, m'} \rangle = C_\ell \delta_{\ell\ell'} \delta_{mm'}$$

and

$$P(a_{\ell\, m}) = \frac{1}{(2\pi C_\ell)^{\frac{2\ell+1}{2}}} \exp\left(-\sum_m \frac{|a_{\ell\, m}|^2}{2C_\ell} \right)$$

Ideal measurement

Warm up: Measurement of temperature anisotropies

For Gaussian perturbations

$$\langle a_{\ell\, m} a^*_{\ell'\, m'} \rangle = C_\ell \delta_{\ell\ell'} \delta_{mm'}$$

and

$$P(a_{\ell\, m}) = \frac{1}{(2\pi C_\ell)^{\frac{2\ell+1}{2}}} \exp\left(-\sum_m \frac{|a_{\ell\, m}|^2}{2C_\ell} \right)$$

So the exact likelihood is

$$\mathcal{L}(\theta) = \prod_\ell \frac{1}{(2\pi C_\ell(\theta))^{\frac{2\ell+1}{2}}} \exp\left(-\sum_m \frac{|a^{\rm obs}_{\ell\, m}|^2}{2C_\ell(\theta)} \right)$$

or for $C_\ell^{\rm obs}$

$$\mathcal{L}(\theta) \propto \prod_\ell \exp\left(-\frac{2\ell+1}{2} \left[\frac{C_\ell^{\rm obs}}{C_\ell(\theta)} + \ln C_\ell(\theta) - \frac{2\ell-1}{2\ell+1} \ln C_\ell^{\rm obs} \right] \right)$$

Ideal measurement

For a measurement including polarization

Define $\mathbf{a}_{\ell\, m} = (a_{T,\ell\, m}, a_{E,\ell\, m}, a_{B,\ell\, m})$

Then $\langle \mathbf{a}_{\ell\, m} \mathbf{a}^\dagger_{\ell'\, m'} \rangle = \mathbf{C}_\ell \delta_{\ell\ell'} \delta_{mm'}$

with $\mathbf{C}_\ell = \begin{pmatrix} C_{TT,\ell} & C_{TE,\ell} & 0 \\ C_{TE,\ell} & C_{EE,\ell} & 0 \\ 0 & 0 & C_{BB,\ell} \end{pmatrix}$

Then the exact likelihood is

$$\mathcal{L}(\theta) = \prod_\ell \frac{1}{(2\pi \det \mathbf{C}_\ell(\theta))^{\frac{2\ell+1}{2}}} \exp\left(-\frac{1}{2} \sum_m \mathbf{a}^{\dagger\,\mathrm{obs}}_{\ell\, m} \mathbf{C}_\ell^{-1}(\theta) \mathbf{a}^{\mathrm{obs}}_{\ell\, m} \right)$$

or

$$\mathcal{L}(\theta) \propto \prod_\ell \frac{(\det \mathbf{C}_\ell^{\mathrm{obs}})^{\frac{2\ell-n}{2}}}{(\det \mathbf{C}_\ell(\theta))^{\frac{2\ell+1}{2}}} \exp\left(-\frac{2\ell+1}{2} \mathrm{tr} \mathbf{C}_\ell^{\mathrm{obs}} \mathbf{C}_\ell^{-1} \right)$$

Parameter estimation

To find the likelihood as function of our parameters, we could evaluate it on a grid.

Since the likelihoods are typically costly to evaluate and especially for higher dimensional parameter spaces this is too time consuming.

We sample them using Markov Chain Monte Carlo methods instead.

Parameter estimation

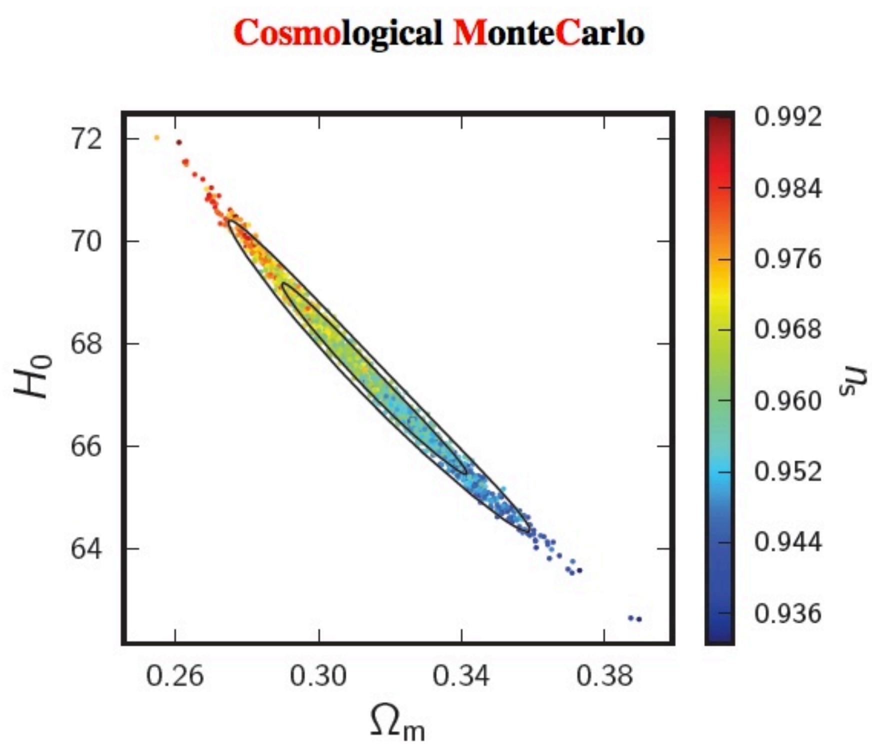

http://cosmologist.info/cosmomc/

http://baudren.github.io/montepython.html

Parameter estimation

Metropolis-Hastings

- Choose a starting point in parameter space and compute $\mathcal{L}(\theta_0)$
- Pick a randomly chosen second point and compute $\epsilon = \mathcal{L}(\theta_1)/\mathcal{L}(\theta_0)$
- If $\epsilon > 1$ keep the point, if $\epsilon < 1$ keep with probability ϵ
- Repeat

With some additional work this will generate random points drawn from $\mathcal{L}(\theta)$, which can be used to find best-fits, means, error bars...

Adding Real World Effects

In realistic measurements, we have to incorporate

- Noise of the experiment
- Finite resolution of the experiment
- Pixelization of maps
- Masks
- ...

Adding Real World Effects

In realistic measurements, we have to incorporate

- Noise of the experiment
- Finite resolution of the experiment
- Pixelization of maps
- Masks
- ...

Notice that these likelihoods are Gaussian in terms of $\mathbf{a}_{\ell\, m}^{\mathrm{obs}}$ but not in terms of $\mathrm{C}_{\ell}^{\mathrm{obs}}$

Incorporating these effects is thus easy in map space where the likelihoods are Gaussian

Adding Real World Effects

Pixel space likelihood

$$\langle \Delta T_i \Delta T_j \rangle = \mathbf{C}_{ij} + \mathbf{N}_{ij}$$

observed pixels

Noise covariance matrix

Pixel covariance for signal

The probability distribution for the ΔT_i is

$$P(\Delta T_i) = \frac{1}{(2\pi)^{N_{\rm pix}/2}\sqrt{\det(\mathbf{C}+\mathbf{N})}} \exp\left(-\frac{1}{2} \sum_{ij} \Delta T_i (\mathbf{C}+\mathbf{N})^{-1}_{ij} \Delta T_j \right)$$

Adding Real World Effects

Pixel space likelihood

So the exact likelihood in pixel space is

$$\mathcal{L}(\theta) = \frac{1}{(2\pi)^{N_{\rm pix}/2}\sqrt{\det(\mathbf{C}(\theta)+\mathbf{N})}} \exp\left(-\frac{1}{2}\sum_{ij}\Delta T_i^{\rm obs}(\mathbf{C}(\theta)+\mathbf{N})_{ij}^{-1}\Delta T_j^{\rm obs}\right)$$

This easily extends to polarization

Adding Real World Effects

Pixel space likelihood

So the exact likelihood in pixel space is

$$\mathcal{L}(\theta) = \frac{1}{(2\pi)^{N_{\rm pix}/2}\sqrt{\det(\mathbf{C}(\theta)+\mathbf{N})}} \exp\left(-\frac{1}{2}\sum_{ij}\Delta T_i^{\rm obs}(\mathbf{C}(\theta)+\mathbf{N})^{-1}_{ij}\Delta T_j^{\rm obs}\right)$$

This easily extends to polarization

Unfortunately evaluating such likelihoods is prohibitively expensive for high resolution full sky experiments such as WMAP or Planck.

To make progress, one uses approximations for the likelihoods based on the $\mathbf{C}_\ell^{\rm obs}$.

Adding Real World Effects

Pseudo-C_ℓ likelihood

One (of many) approximations is a fiducial Gaussian approximation (used by Planck)

$$\mathcal{L}(\theta) \propto \frac{1}{\sqrt{\det(\mathcal{C}_{\text{fid}})}} \exp\left[-\frac{1}{2}(\mathbf{C}^{\text{obs}} - \mathbf{C}(\theta))^t \mathcal{C}_{\text{fid}}^{-1} (\mathbf{C}^{\text{obs}} - \mathbf{C}(\theta))\right]$$

with covariance matrix $\mathcal{C}_{\text{fid}} = \langle \mathbf{C}\mathbf{C}^t \rangle$ evaluated for some fiducial cosmology close to the true cosmology.

The covariance matrix can be computed analytically even for masked maps and in the presence of noise

Adding Real World Effects

Spectra and covariance for pseudo-C_ℓ likelihood

For masked sky maps

$$\Delta\tilde{T}_i^a = W_i^a(\Delta T_i^a + N_i^a)$$

we have multipole coefficients

$$\tilde{a}_{\ell m}^a = \sum_i \Omega_i \Delta\tilde{T}_i^a Y_{\ell m}^*(\hat{n}_i)$$

and pseudo-spectra

$$\tilde{C}_\ell^{ab} \equiv \frac{1}{2\ell+1}\sum_m \tilde{a}_{\ell m}^a \tilde{a}_{\ell m}^{b*}$$

These are related to the underlying power spectra by

$$\langle \tilde{C}_\ell^{ab} \rangle = \sum_{\ell'} M_{\ell\ell'}^{ab}(p_{\ell'} b_{\ell'}^{ab})^2 \langle \hat{C}_{\ell'}^{ab} \rangle + \tilde{N}_\ell^{ab}$$

Adding Real World Effects

Spectra and covariance for pseudo-C_ℓ likelihood

For masked sky maps

$$\Delta\tilde{T}_i^a = W_i^a(\Delta T_i^a + N_i^a)$$

we have multipole coefficients

$$\tilde{a}_{\ell m}^a = \sum_i \Omega_i \Delta\tilde{T}_i^a Y_{\ell m}^*(\hat{n}_i)$$

and pseudo-spectra

$$\tilde{C}_\ell^{ab} \equiv \frac{1}{2\ell+1}\sum_m \tilde{a}_{\ell m}^a \tilde{a}_{\ell m}^{b*}$$

These are related to the underlying power spectra by

$$\langle \tilde{C}_\ell^{ab} \rangle = \sum_{\ell'} M_{\ell\ell'}^{ab} (p_{\ell'} b_{\ell'}^{ab})^2 \langle \hat{C}_{\ell'}^{ab} \rangle + \tilde{N}_\ell^{ab}$$

beam

mode coupling matrix

pixel window function

Adding Real World Effects

Spectra and covariance for pseudo-C_ℓ likelihood

Their covariance matrix is

$$\begin{aligned}
\langle \Delta \tilde{C}_\ell^{ab} \Delta \tilde{C}_{\ell'}^{cd} \rangle &= \sqrt{C_\ell^{ac} C_\ell^{bd} C_{\ell'}^{ac} C_{\ell'}^{bd}}\, \Xi(\ell, \ell', W^{(ac)(bd)}) + \sqrt{C_\ell^{ad} C_\ell^{bc} C_{\ell'}^{ad} C_{\ell'}^{bc}}\, \Xi(\ell, \ell', W^{(ad)(bc)}) \\
&+ \sqrt{C_\ell^{ac} C_{\ell'}^{ac}}\, \Xi(\ell, \ell', W_\sigma^{(ac)(bd)}) + \sqrt{C_\ell^{ad} C_{\ell'}^{ad}}\, \Xi(\ell, \ell', W_\sigma^{(ad)(bc)}) \\
&+ \sqrt{C_\ell^{bd} C_{\ell'}^{bd}}\, \Xi(\ell, \ell', W_\sigma^{(bd)(ac)}) + \sqrt{C_\ell^{bc} C_{\ell'}^{bc}}\, \Xi(\ell, \ell', W_\sigma^{(bc)(ad)}) \\
&+ \Xi(\ell, \ell', W_{\sigma\sigma}^{(ac)(bd)}) + \Xi(\ell, \ell', W_{\sigma\sigma}^{(ad)(bc)})
\end{aligned}$$

with

$$\begin{aligned}
W_\ell^{(ac)(bd)} &= \frac{1}{2\ell+1} \sum_m w_{\ell m}^{ac} w_{\ell m}^{bd*}\,, \\
W_{\sigma\,\ell}^{(ac)(bd)} &= \frac{1}{2\ell+1} \sum_m w_{\ell m}^{ac} w_{\sigma\,\ell m}^{bd*}\,, \\
W_{\sigma\sigma\,\ell}^{(ac)(bd)} &= \frac{1}{2\ell+1} \sum_m w_{\sigma\,\ell m}^{ac} w_{\sigma\,\ell m}^{bd*}\,,
\end{aligned}$$

$$\begin{aligned}
w_{\ell m}^{ab} &= \sum_i \Omega_i W_i^a W_i^b Y_{\ell m}^*(\hat{n}_i)\,, \\
w_{\sigma\,\ell m}^{ab} &= \sum_i \Omega_i^2 W_i^{a2} \sigma_i^{a2} \delta^{ab} Y_{\ell m}^*(\hat{n}_i)\,.
\end{aligned}$$

Adding Real World Effects

Hybrid likelihoods

Pixel based likelihoods are exact but prohibitively expensive for full sky, high resolution experiments

Pseudo-C_ℓ likelihood only accurate for high enough multipoles as the C_ℓ obey a χ-square distribution with $2\ell + 1$ degrees of freedom

This suggests using a hybrid likelihood consisting of a pixel based likelihood on large scales and a pseudo-C_ℓ likelihood on small scales

WMAP

- Launched on June 30, 2001
- Observed "from" L2
- End of observations August 2010

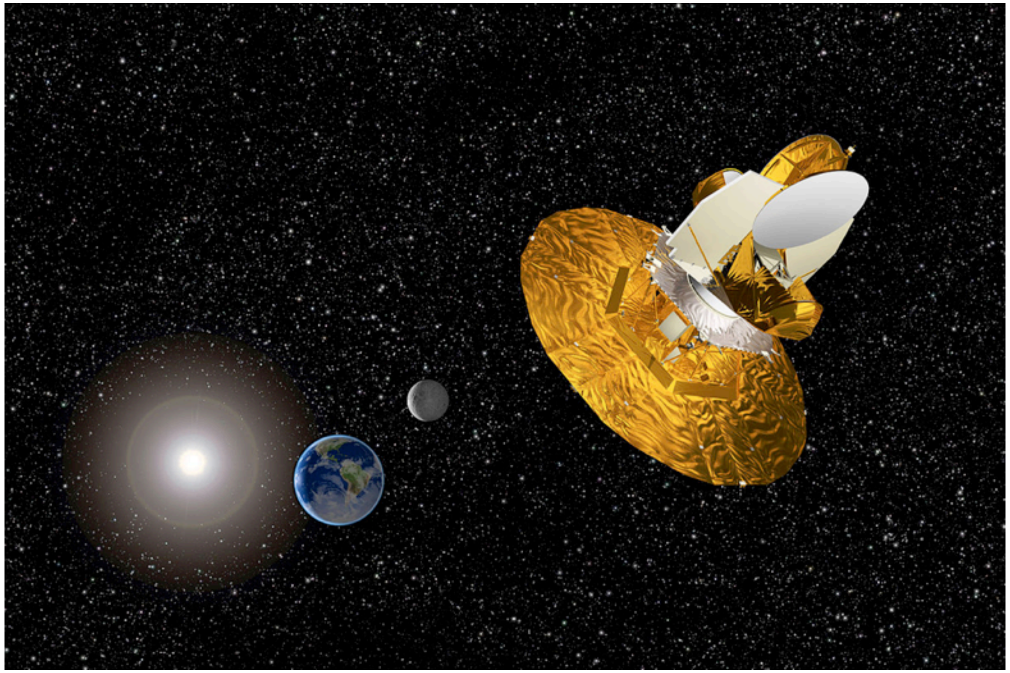

WMAP data

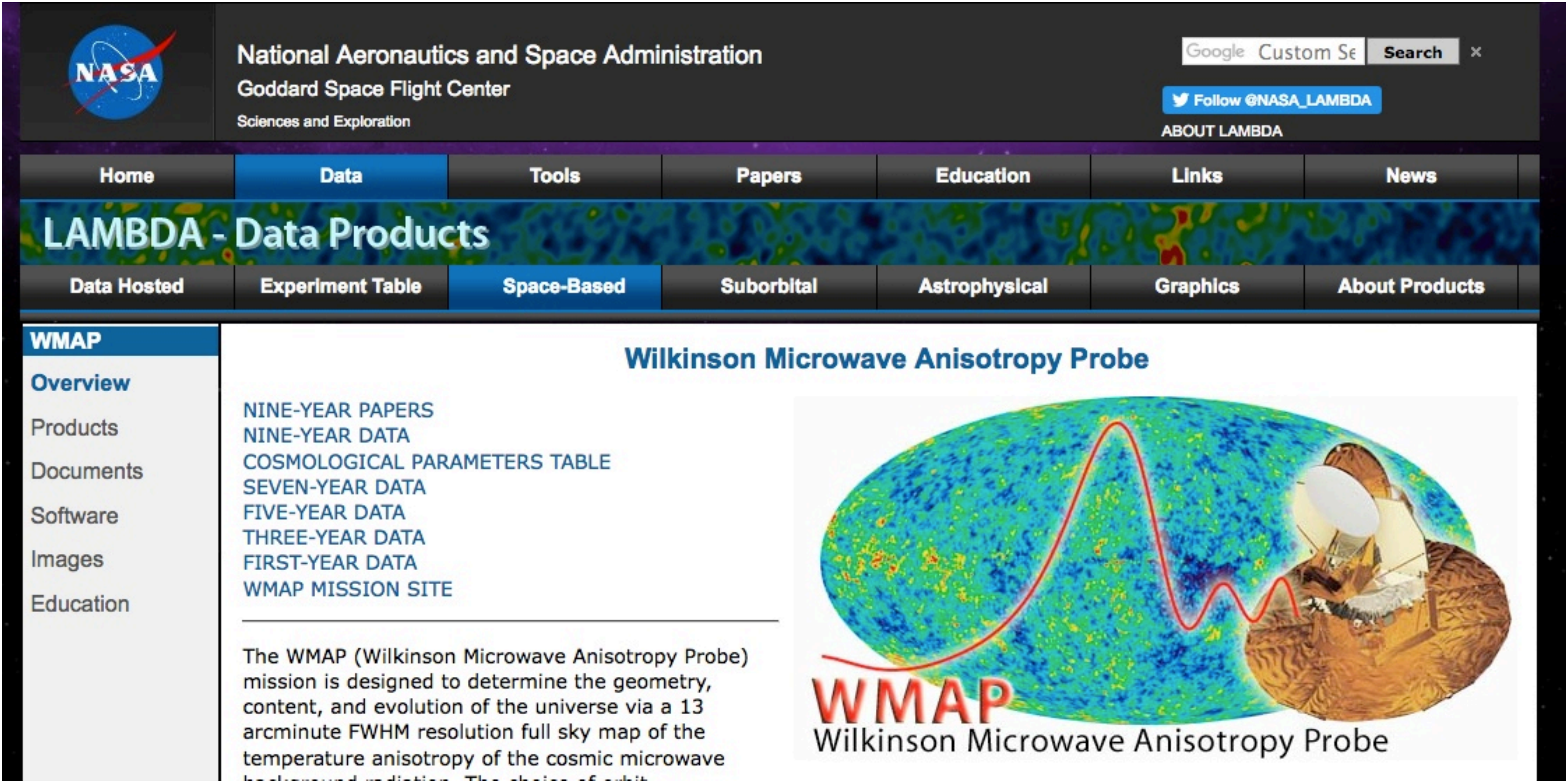

https://lambda.gsfc.nasa.gov/product/map/dr5/

WMAP data

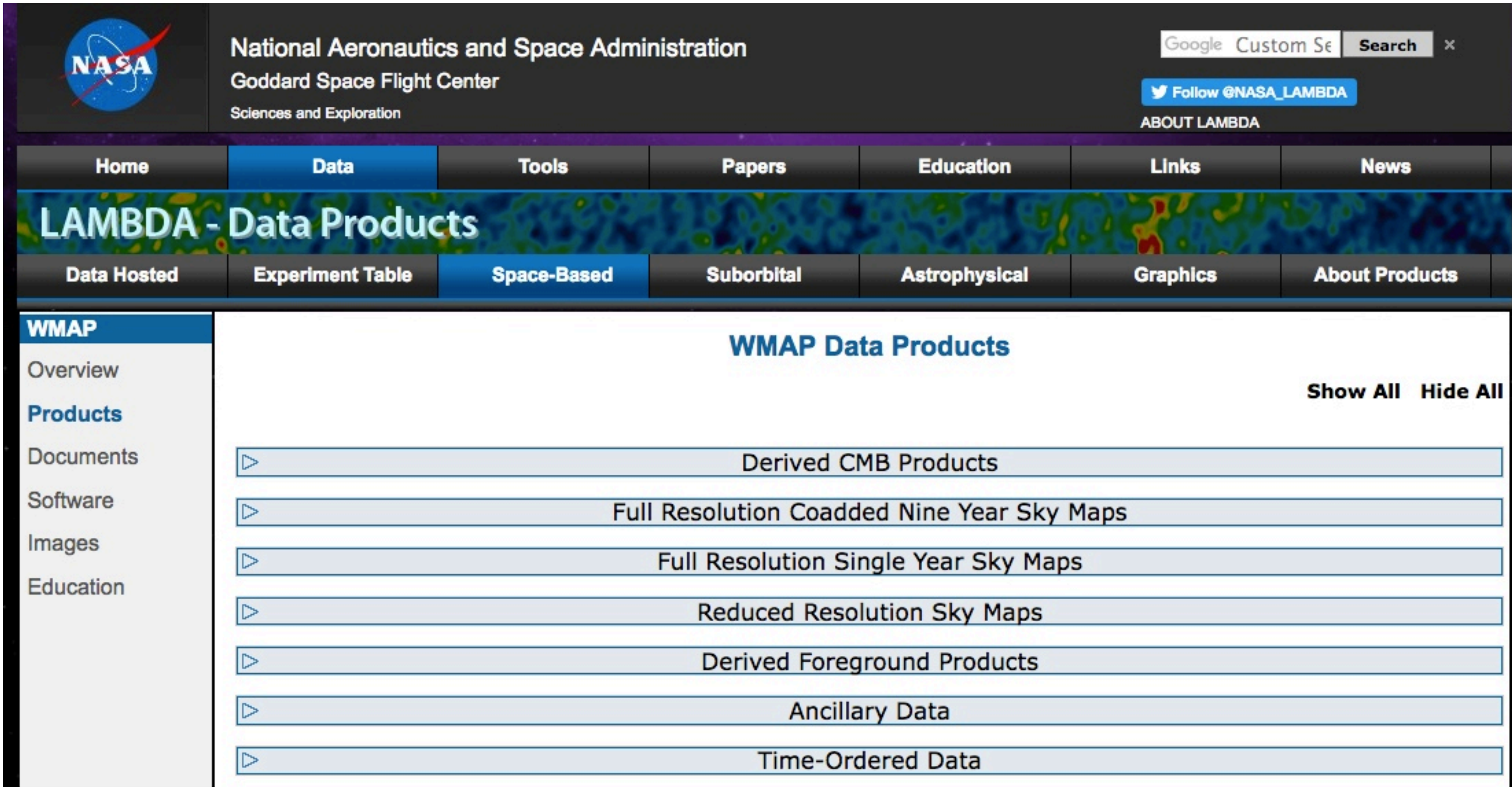

https://lambda.gsfc.nasa.gov/product/map/dr5/

Planck

- Launched on May 14, 2009
- Observed "from" L2 from August 12, 2009
- End of observations for HFI January 2012
- End of observations for LFI August 2013
- Temperature data for "nominal" mission released on March 21, 2013

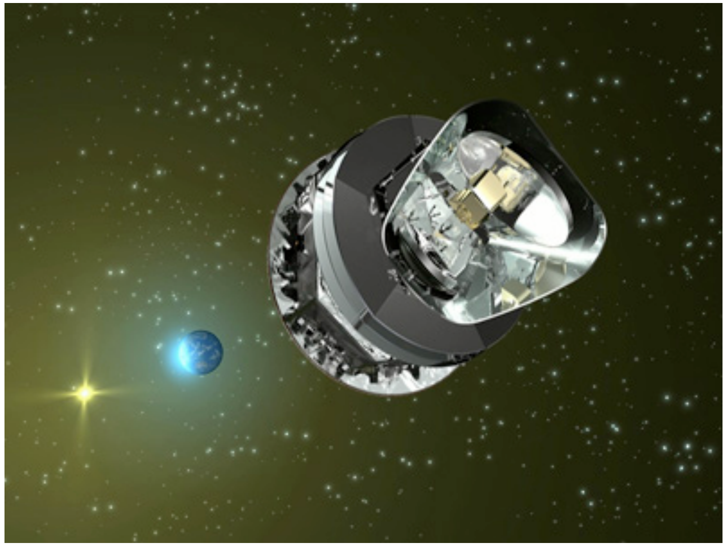

- First release of full mission data on February 5, 2015

Planck data

NASA/IPAC INFRARED SCIENCE ARCHIVE

IRSA | DATA SETS | SEARCH | TOOLS | HELP

Planck Public Data Release 2 Maps

Primary maps

Planck All Sky Maps are in HEALPix format, with Nside 1024 or 2048, in Galactic coordinates, and nested ordering. The signal is given in units of K_{cmb} for 30-353 GHz, or MJy/sr (for a constant νF_ν energy distribution) for 545 and 857 GHz.

Unpolarized maps contain 3 planes, labeled I_Stokes (intensity), Hits (hit count), and II_cov (variance of I_Stokes).

Polarized maps contain 10 planes, labeled I_Stokes (intensity), Q_Stokes and U_Stokes (linear polarization), Hits (hit count), II_cov, QQ_cov, and UU_cov (variance of each of the Stokes parameters), and IQ_cov, IU_cov, and QU_cov (covariances between the Stokes parameters).

The **Pink** cells indicate maps with polarization data, while the **Blue** cells are the maps with no polarization data.

The LFI maps in this matrix have not been bandpass corrected. Bandpass corrected LFI maps are available at the bottom of the page

Download a script to download all the maps in this table. You can edit the script as needed to select the maps to download.

Planck Primary Maps										
	LFI				HFI					
Frequency (GHz)	030	044	070	070	100	143	217	353	545	857
Nside	1024	1024	1024	2048	2048	2048	2048	2048	2048	2048
Full mission maps										

https://irsa.ipac.caltech.edu/data/Planck/release_2/

Planck data

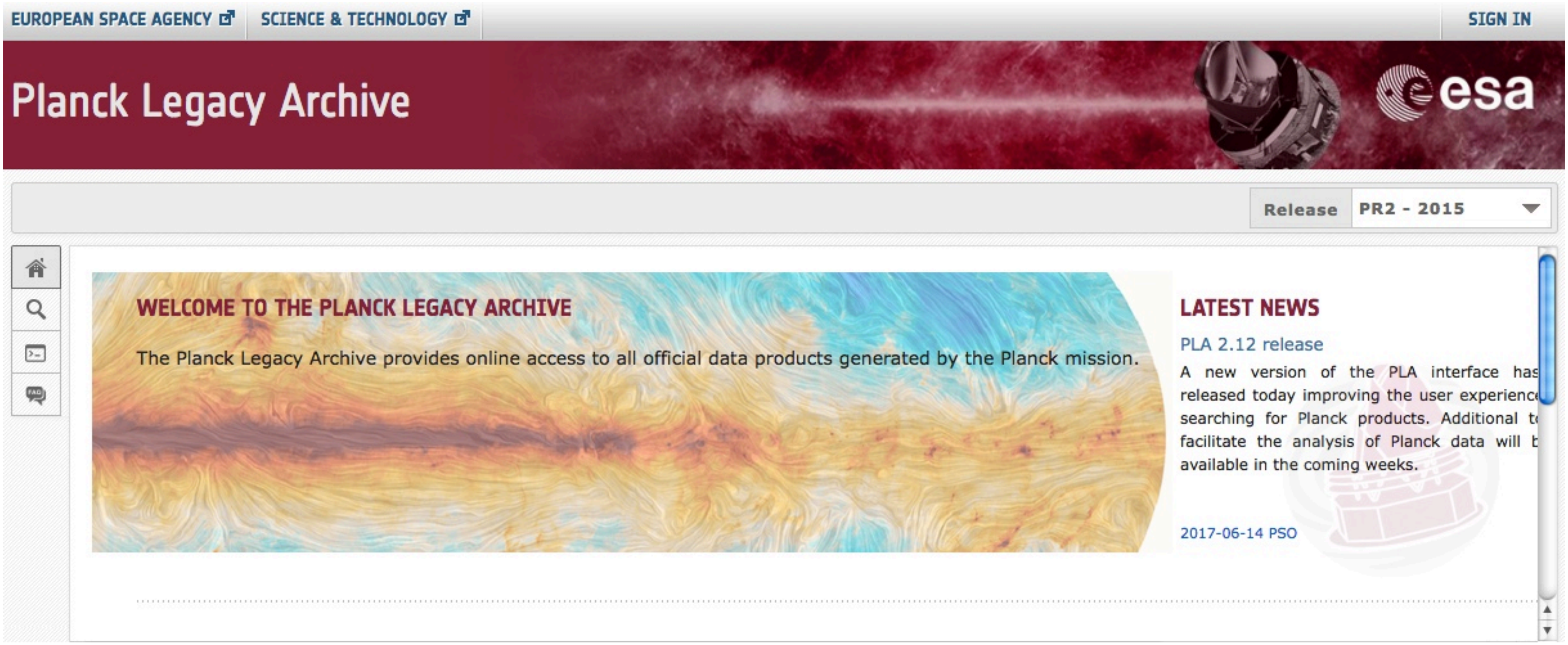

http://pla.esac.esa.int/pla/#home

Planck & WMAP

- Planck and WMAP temperature data agree very well at WMAP resolution

WMAP 94 GHz

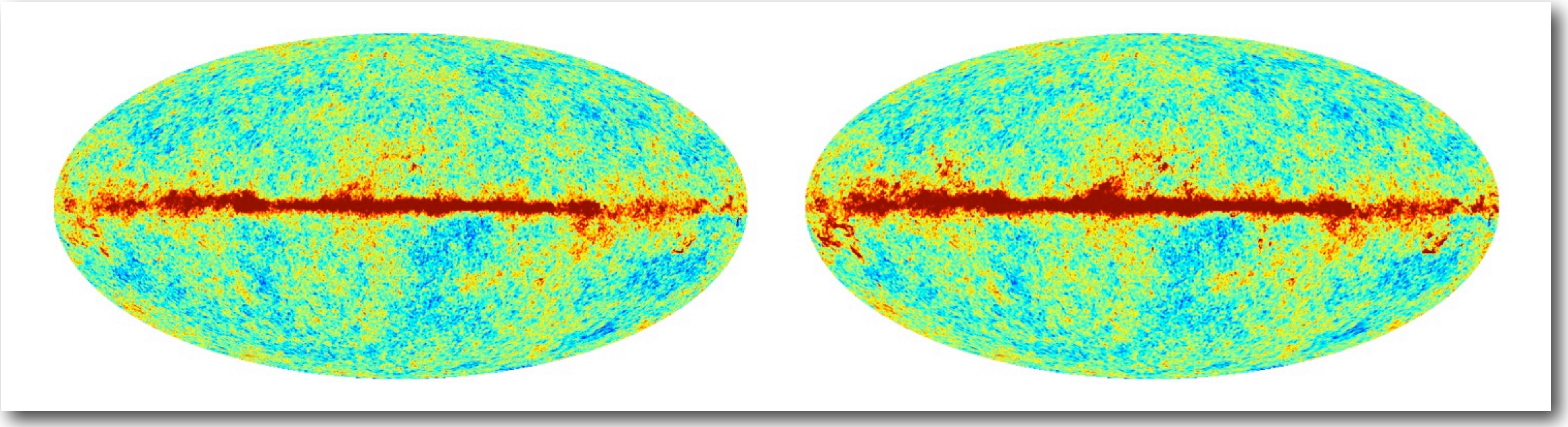

(N_{side}=512)

Planck & WMAP

Planck 100 GHz

- WMAP 94 GHz =

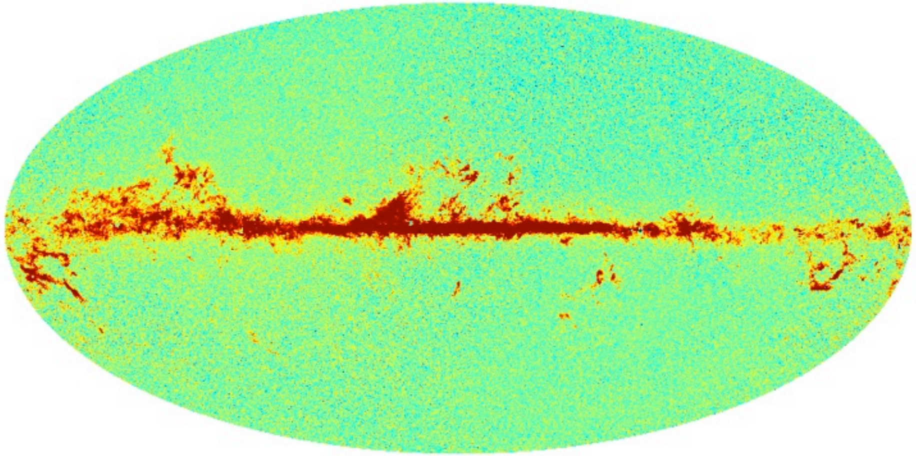

Planck & WMAP

The small but visible difference is due to a CO emission line

Planck 100 GHz

- WMAP 94 GHz =

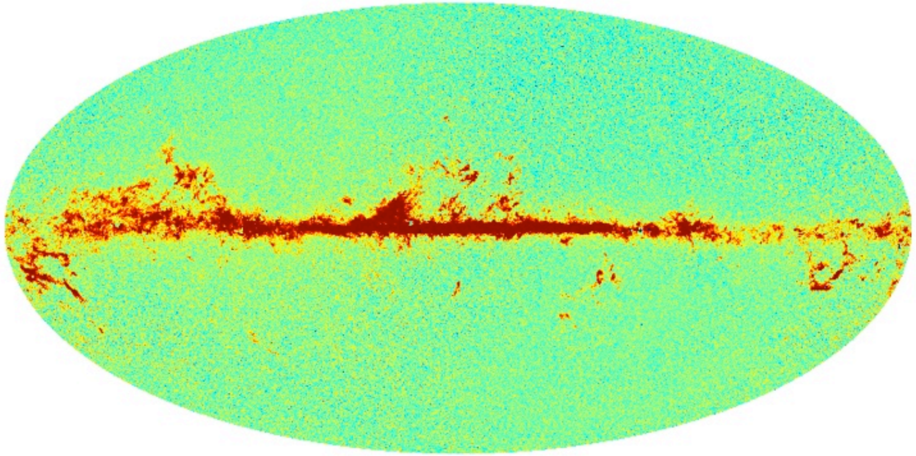

vs Planck CO$(1-0)$ map

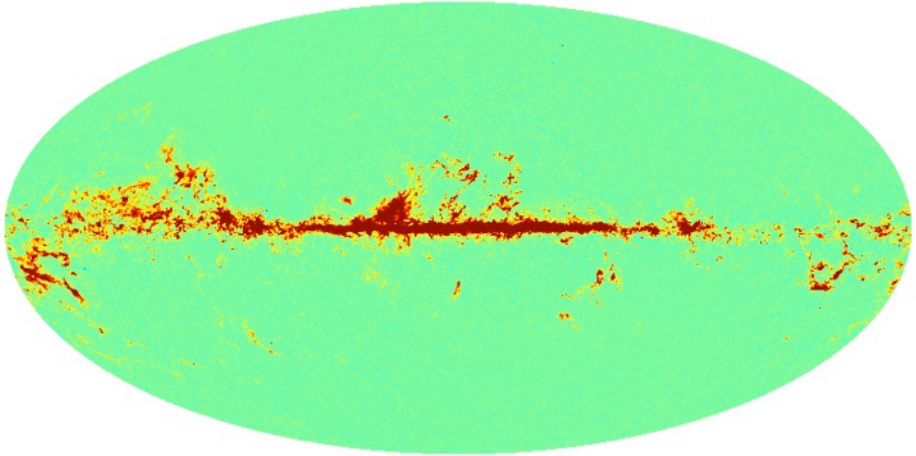

Planck & WMAP

- Planck and WMAP temperature data agrees very well at WMAP resolution
- Planck is much more powerful

WMAP 94 GHz　　　Planck 100 GHz

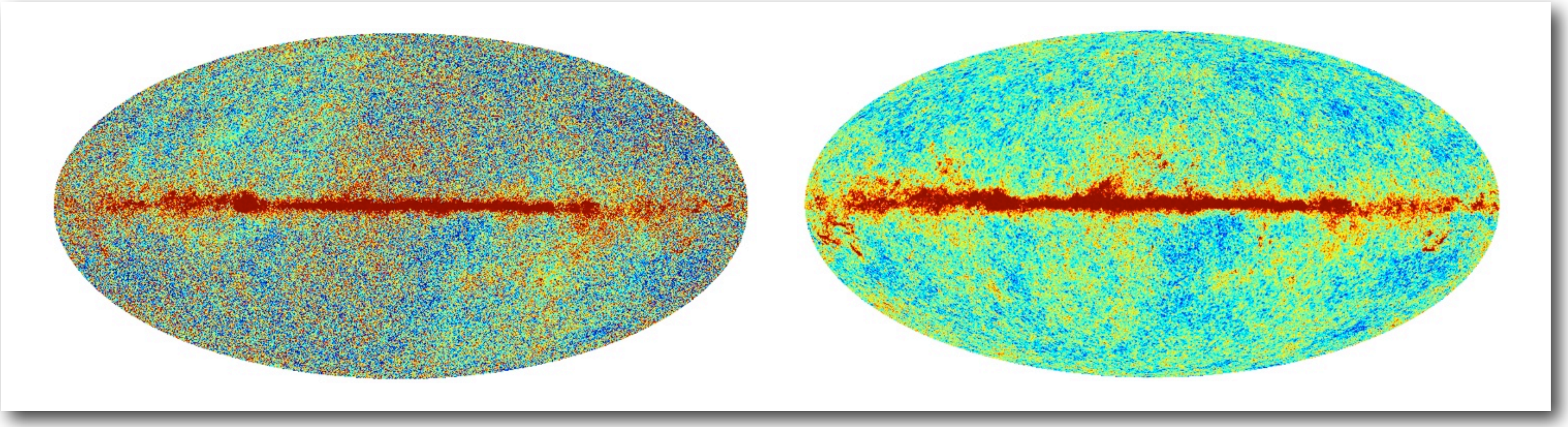

(N_{side}=1024)

Planck & WMAP

- Planck and WMAP temperature data agrees very well at WMAP resolution
- Planck is much more powerful

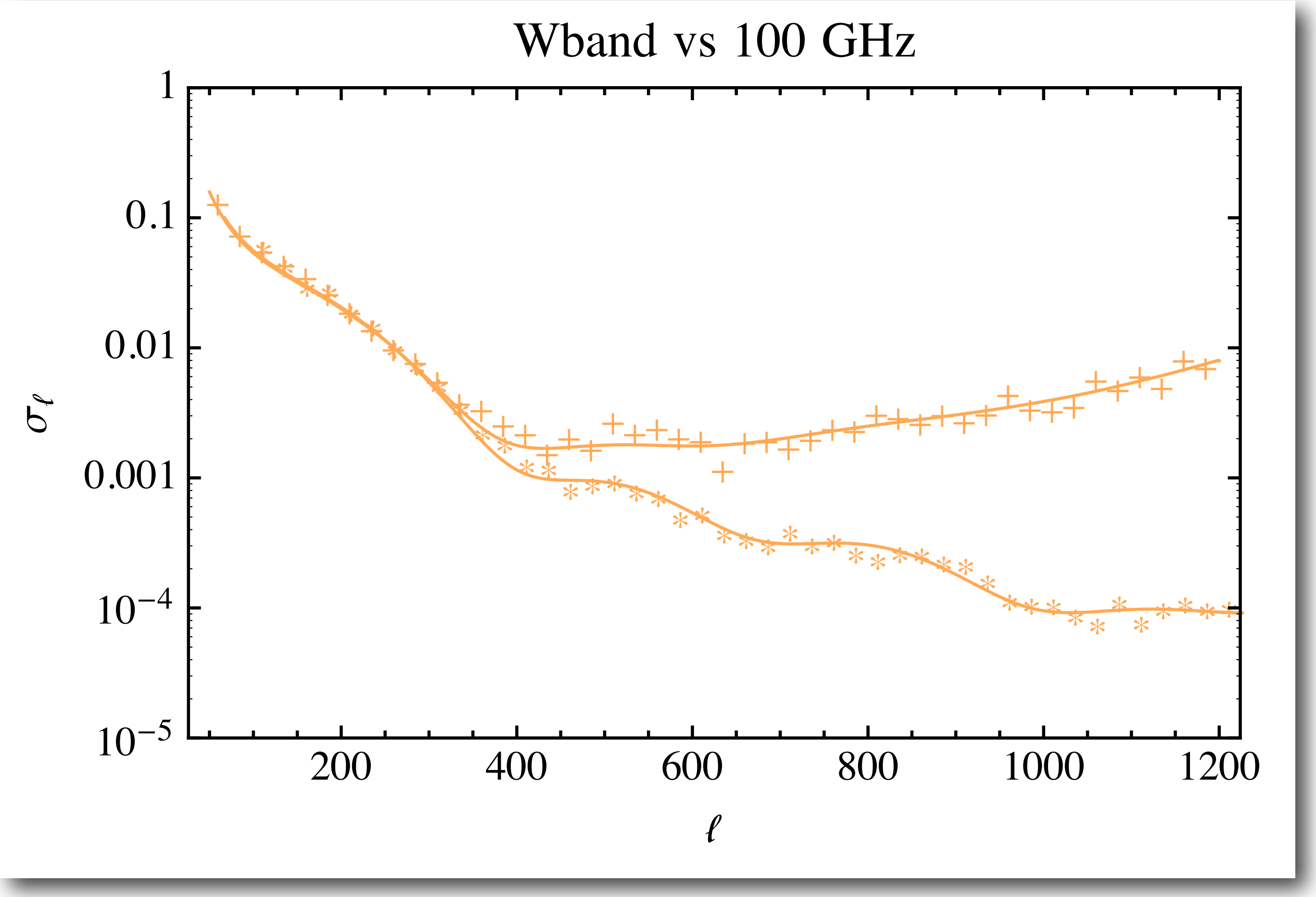

Beyond WMAP and Planck

Home | Data | Tools | Papers | Education | Links | News

LAMBDA - Data Products

Data Hosted | Experiment Table | Space-Based | Suborbital | Astrophysical | Graphics | About Products

Data Hosted on LAMBDA

Below is a list of CMB experiments, with links to internal LAMBDA pages which provide the publicly available data from these experiments. LAMBDA serves as a long-term repository for these archives. If an experiment of interest to you is missing from the list, or there is experimental data you would like to provide, please contact us via the suggestion form. A discussion of the polarization convention used in the datasets can be seen at our polarization convention page.

Cosmic Microwave Background Anisotropy Experiments

ACT	Atacama Cosmology Telescope (Temperature and Polarization)
BICEP2/Keck	Background Imaging of Cosmic Extragalactic Polarization 2/Keck Array
Planck	Planck Mission
POLARBEAR	POLARization of Background microwave Radiation
QUIET	Q/U Imaging ExperimenT
SPT	South Pole Telescope (Temperature and Polarization)
WMAP	Wilkinson Microwave Anisotropy Probe

Cosmic Microwave Background Spectrum Experiments

ARCADE	Absolute Radiometer for Cosmology, Astrophysics, and Diffuse Emission
COBE-FIRAS	Cosmic Background Explorer
TRIS	Three Radiometer CMB Spectrum Experiment

Planck Angular Power Spectrum

The likelihood is a hybrid of a

- pixel space likelihood for low ℓ
  (T mostly constrains amplitude, P mostly constrains optical depth)
- fiducial Gaussian approximation for high ℓ

	2013	2015
low-ℓ T	Commander ($f_{\rm sky} = 0.87$)	Commander ($f_{\rm sky} = 0.93$)
low-ℓ P	WMAP($f_{\rm sky} = 0.76$)	Planck LFI($f_{\rm sky} = 0.47$)
high-ℓ	CAMspec	Plik

Planck Angular Power Spectrum

The high-ℓ likelihoods are based on

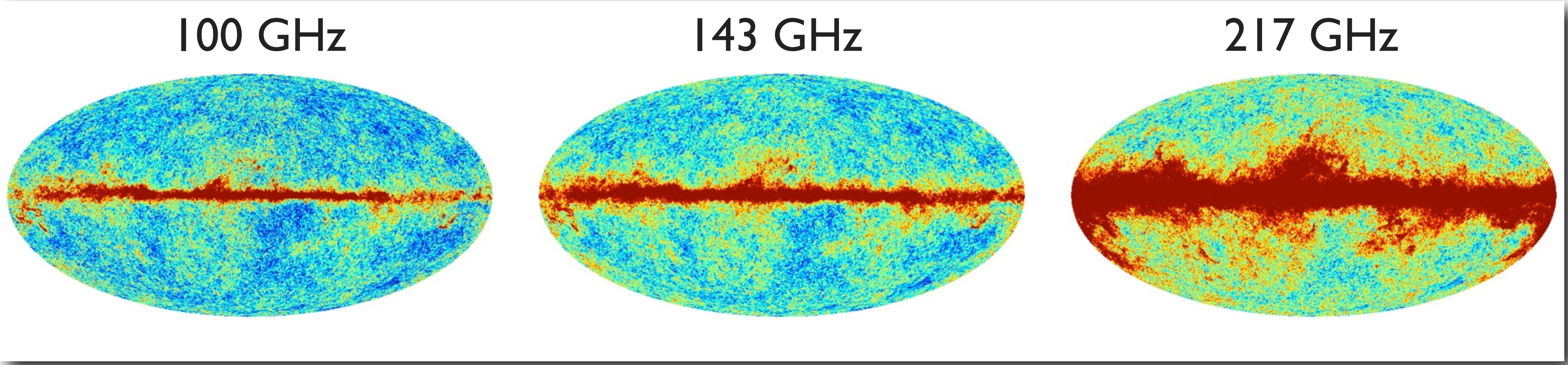

- 100x100 spectra up to $\ell = 1200$
- 143x143 spectra up up to $\ell = 2000$
- 143x217 and 217x217 spectra up to $\ell = 2500$

Planck Angular Power Spectrum

- masks for galactic and point source and CO emission

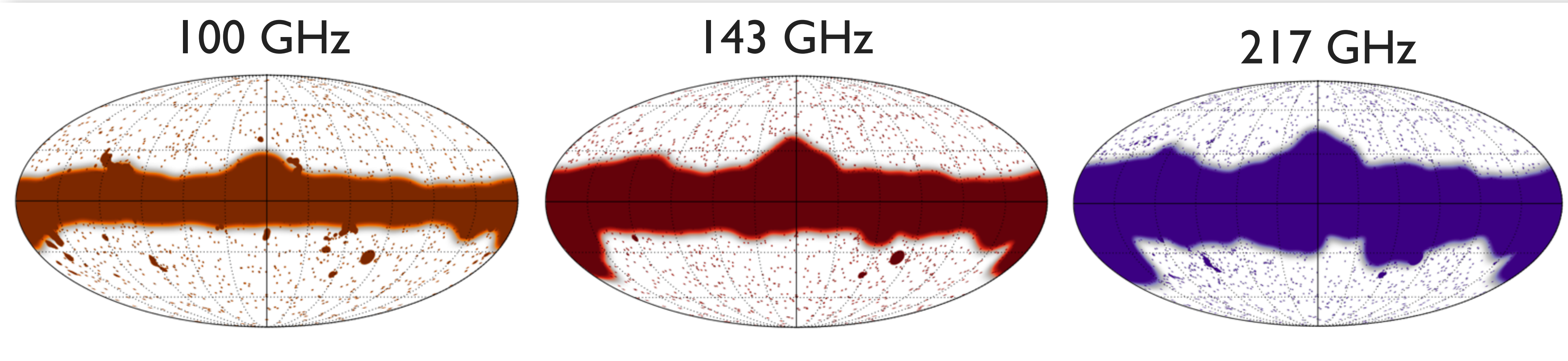

- power spectrum templates to model diffuse galactic emission and extragalactic foregrounds
- analytic, fiducial Gaussian approximation for likelihood as discussed earlier
- noise properties from fit of Planck noise model to map half-differences

Planck Angular Power Spectrum

Noise from half-mission differences

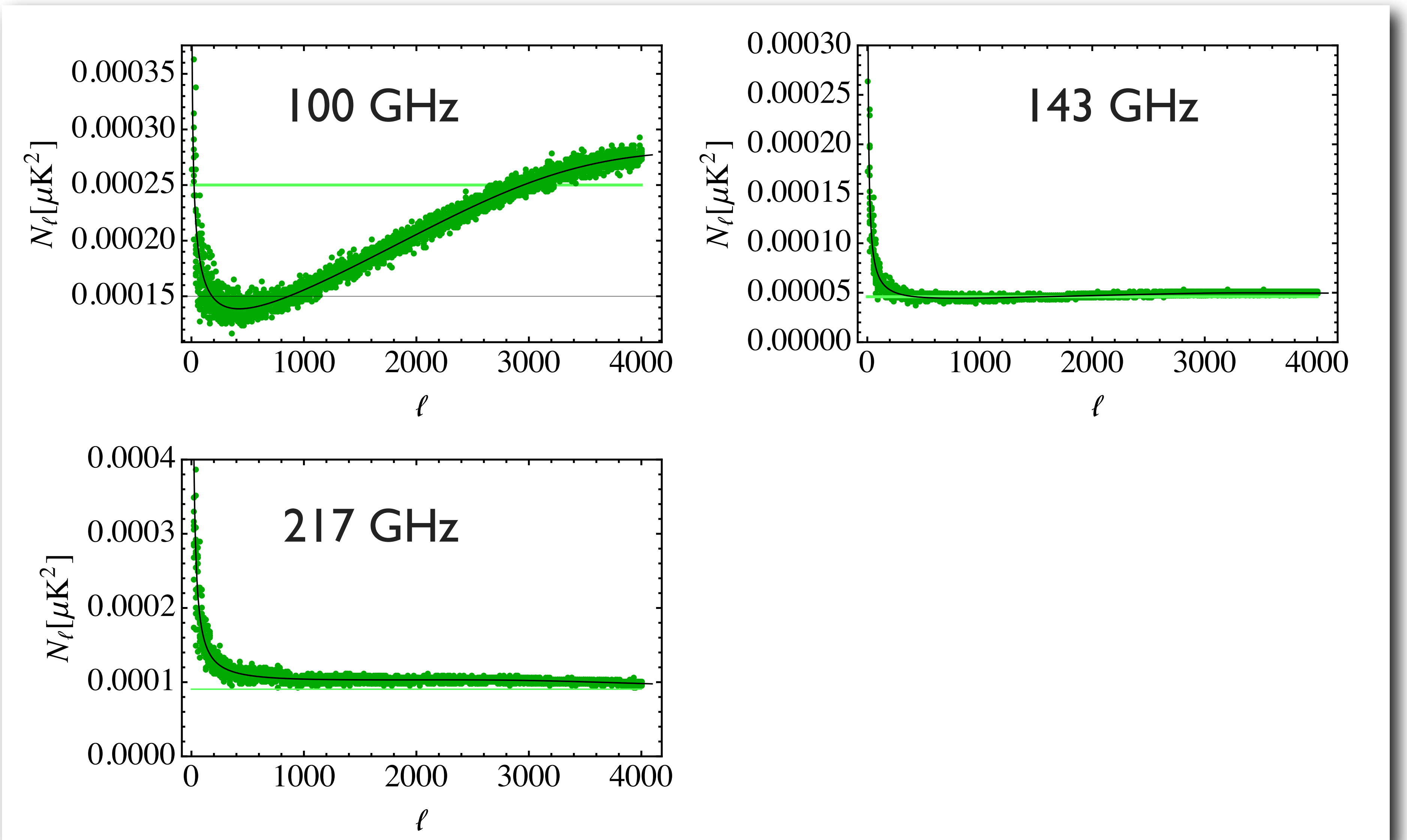

Planck Angular Power Spectrum

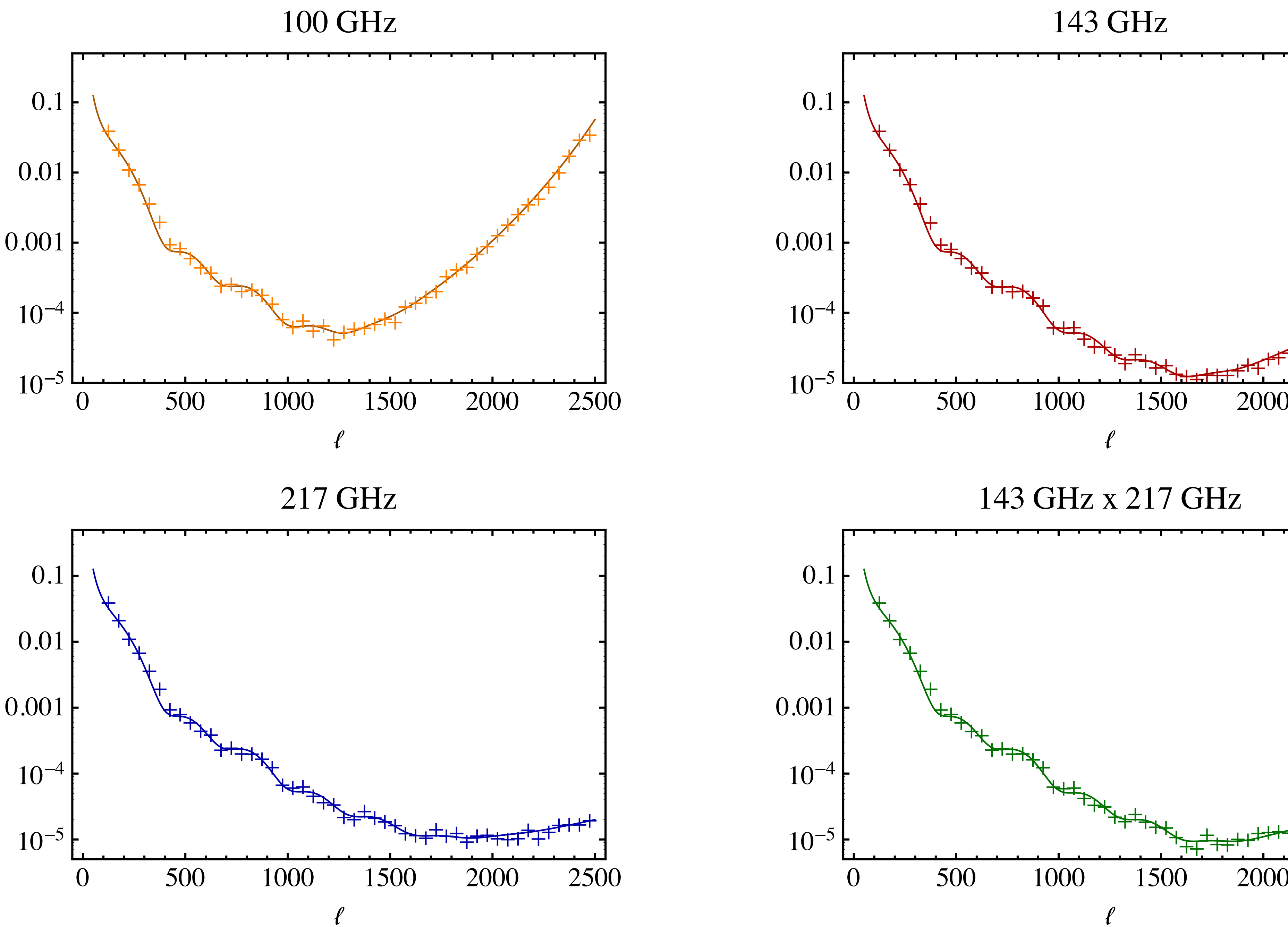

LCDM

Once we have produced a likelihood, we can run our favorite Markov Chain Monte Carlo routine

Parameter	*Planck* TT+lowP
$\Omega_b h^2$	0.02222 ± 0.00023
$\Omega_c h^2$	0.1197 ± 0.0022
$100\theta_{MC}$	1.04085 ± 0.00047
τ	0.078 ± 0.019
$\ln(10^{10} A_s)$	3.089 ± 0.036
n_s	0.9655 ± 0.0062
H_0	67.31 ± 0.96
Ω_m	0.315 ± 0.013
σ_8	0.829 ± 0.014
$10^9 A_s e^{-2\tau}$	1.880 ± 0.014

Gravitational waves and B-modes

Inflation predicts a nearly scale invariant spectrum of gravitational waves

$$\dot{\tilde{\Delta}}^{(T)}_{T,\ell}(q,t) + \frac{q}{a(2\ell+1)}\left[(\ell+1)\tilde{\Delta}^{(T)}_{T,\ell+1}(q,t) - \ell\tilde{\Delta}^{(T)}_{T,\ell-1}(q,t)\right]$$

$$= \left(-2\dot{\mathcal{D}}_q(t) + \omega_c(t)\Psi(q,t)\right)\,\delta_{\ell,0} - \omega_c(t)\tilde{\Delta}^{(T)}_{T,\ell}(q,t)$$

$$\dot{\tilde{\Delta}}^{(T)}_{P,\ell}(q,t) + \frac{q}{a(2\ell+1)}\left[(\ell+1)\tilde{\Delta}^{(T)}_{P,\ell+1}(q,t) - \ell\tilde{\Delta}^{(T)}_{P,\ell-1}(q,t)\right]$$

$$= -\omega_c(t)\Psi(q,t)\,\delta_{\ell,0} - \omega_c(t)\tilde{\Delta}^{(T)}_{P,\ell}(q,t)$$

with

$$\Psi(q,t) = \frac{1}{10}\tilde{\Delta}^{(T)}_{T,0}(q,t) + \frac{1}{7}\tilde{\Delta}^{(T)}_{T,2}(q,t) + \frac{3}{70}\tilde{\Delta}^{(T)}_{T,4}(q,t)$$

$$-\frac{3}{5}\tilde{\Delta}^{(T)}_{P,0}(q,t) + \frac{6}{7}\tilde{\Delta}^{(T)}_{P,2}(q,t) - \frac{3}{70}\tilde{\Delta}^{(T)}_{P,4}(q,t)$$

Gravitational waves and B-modes

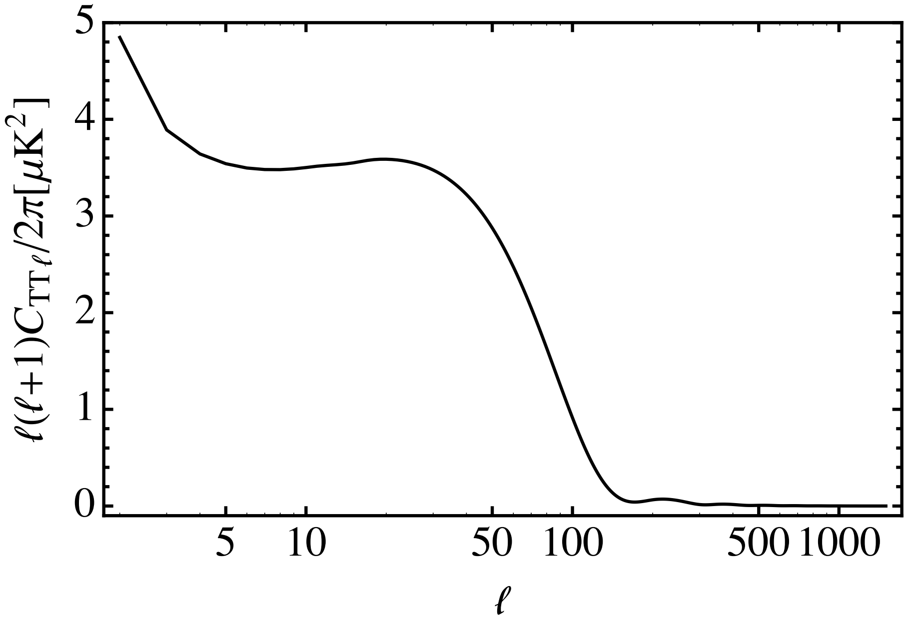

In addition to TT, TE, EE, primordial gravitational waves generate BB

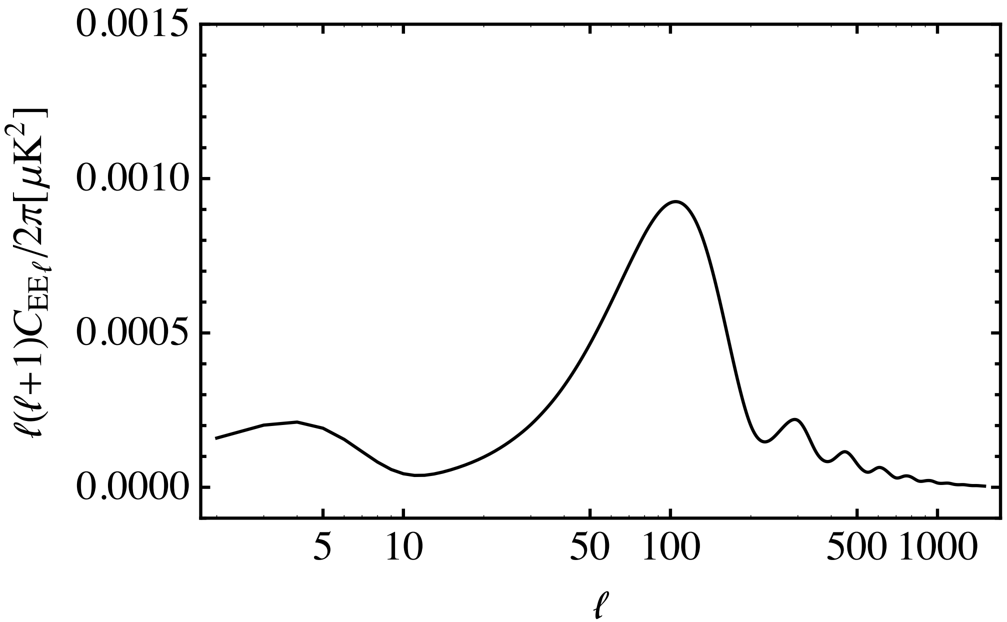

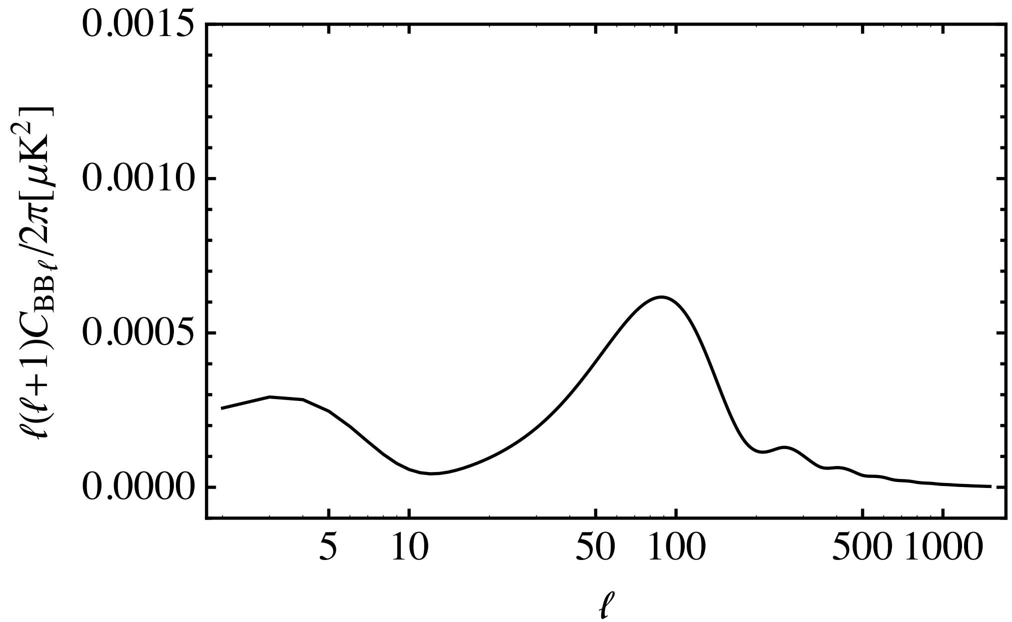

B-mode search

BICEP2 polarization data

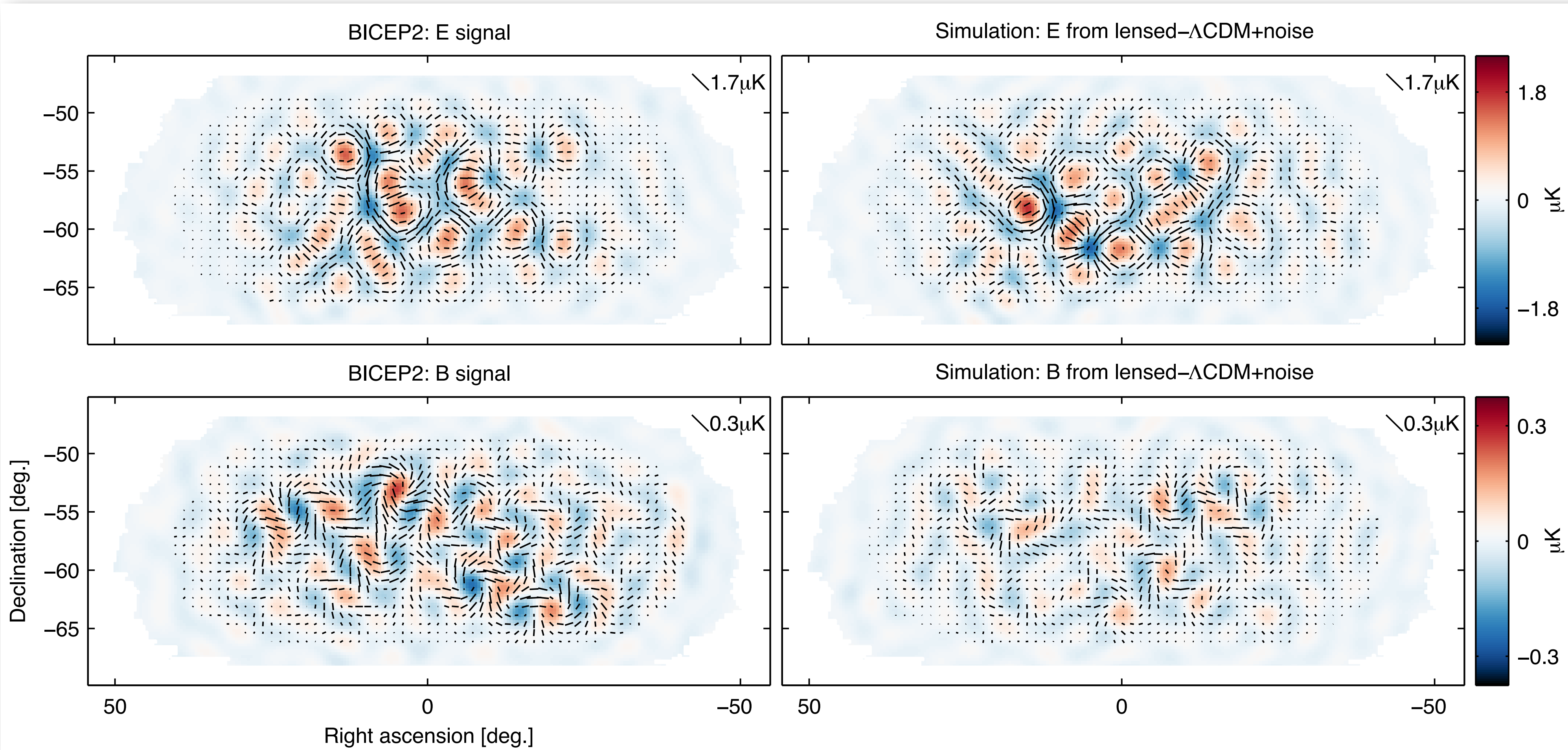

Noise level: 87 nK deg - the deepest map at 150 GHz of this patch of sky

(Planck noise level: few μK deg)

B-mode search

Foreground models made in collaboration with David Spergel, Colin Hill, and Aurelien Fraisse

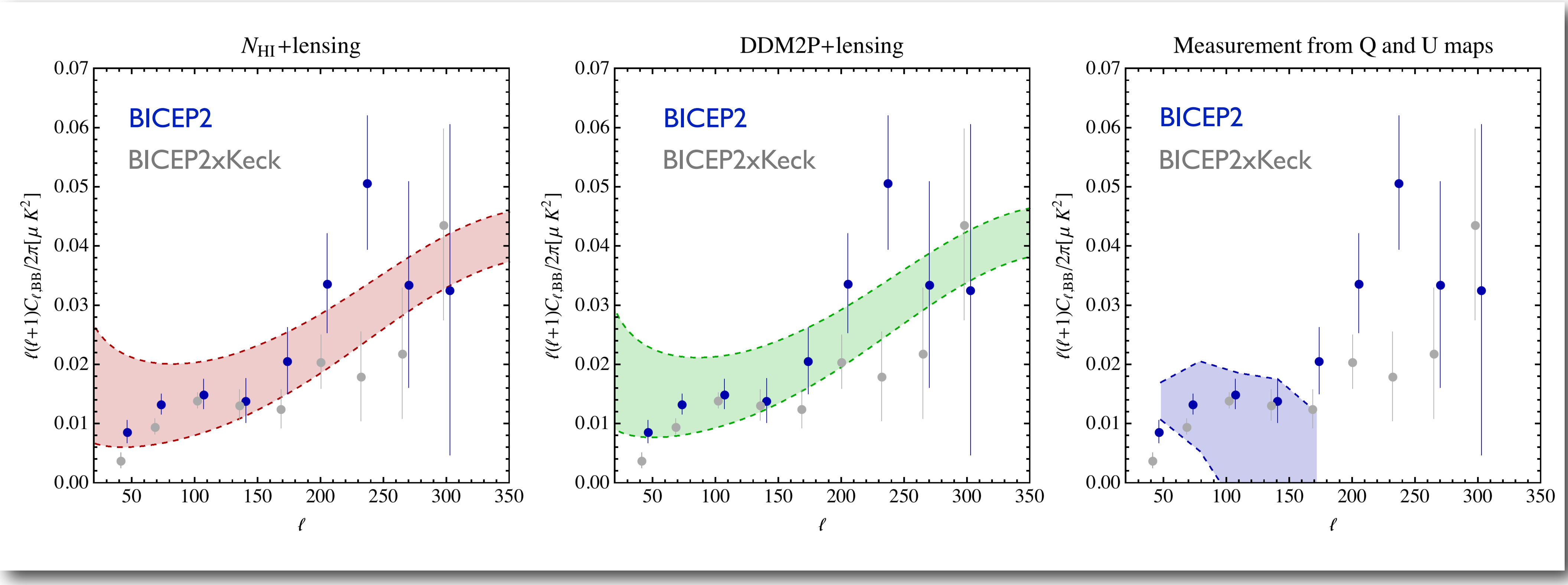

B-mode search

- measurement of BB in the BICEP2 region at 353 GHz rescaled to 150 GHz

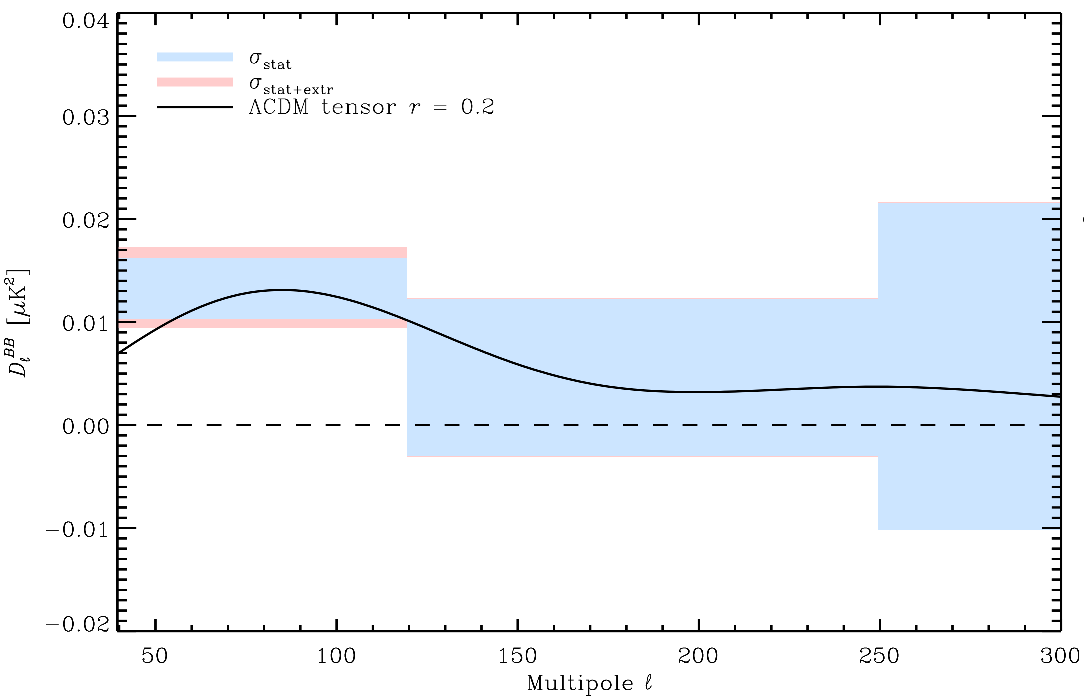

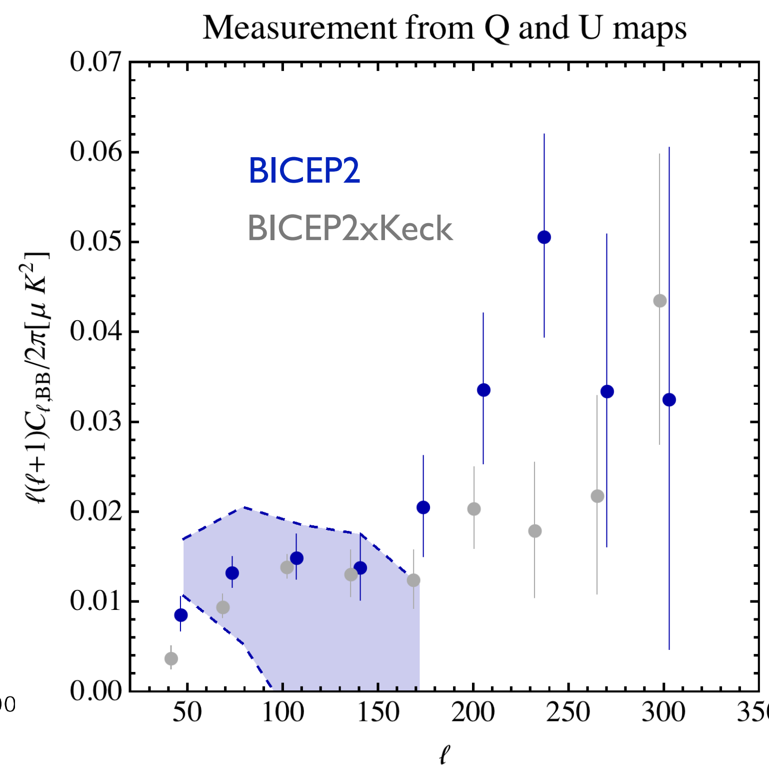

$$D_\ell^{BB} = 1.32\times10^{-2}\,\mu{\rm K}^2_{\rm CMB}$$

B-mode search

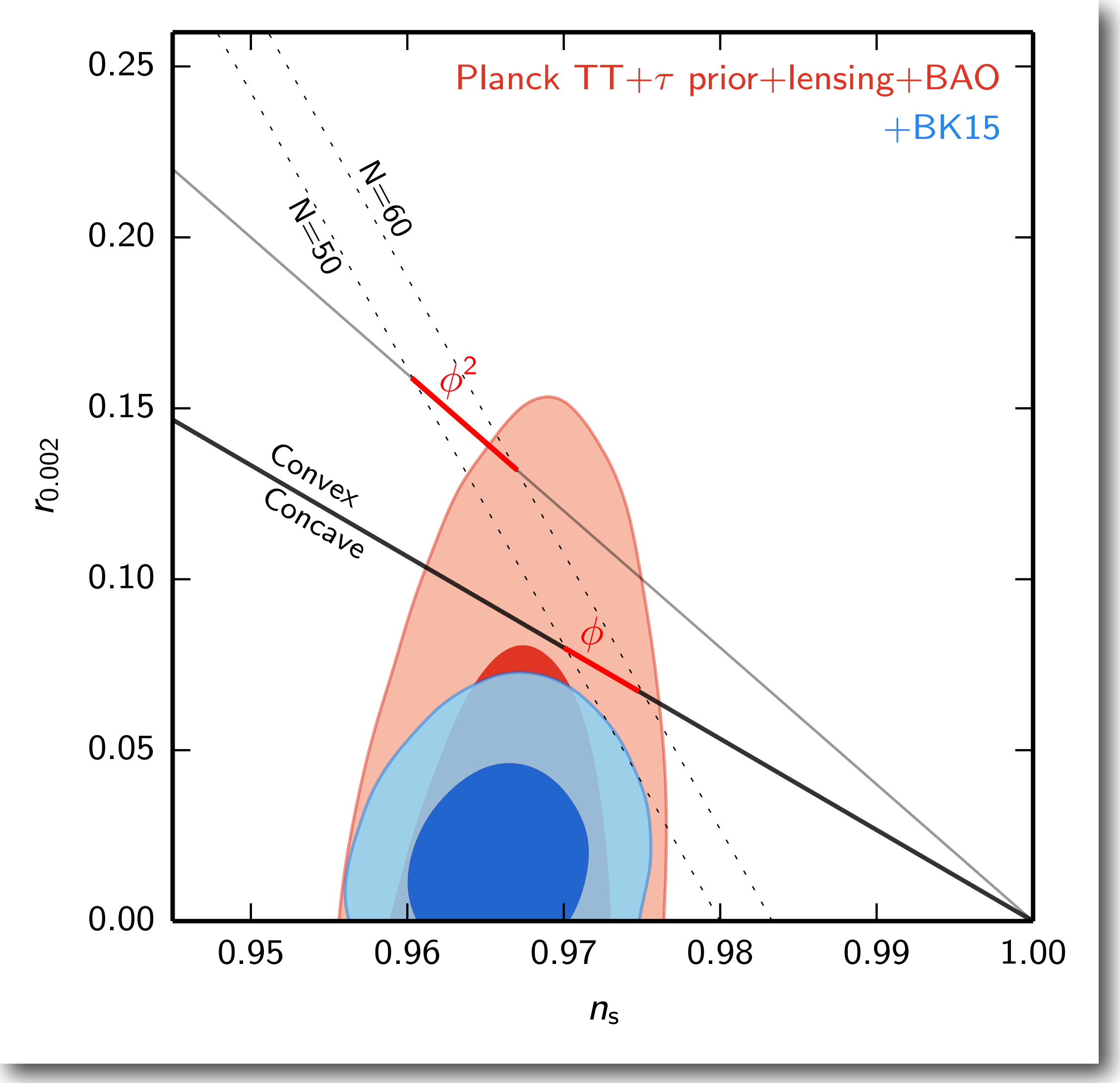

B-mode search

With the current data, we can constrain r by

- the tensor contribution to the temperature anisotropies on large angular scales
- the B-mode polarization generated by tensors.

The two likelihood are essentially independent

$$\mathcal{L}(r_{TT}, r_{BB}) = \mathcal{L}_{TT}(r_{TT})\mathcal{L}_{BB}(r_{BB})$$

Typically we talk about $\mathcal{L}(r, r)$

B-mode search

$\mathcal{L}(r_{TT}, r_{BB})$ before BICEP2

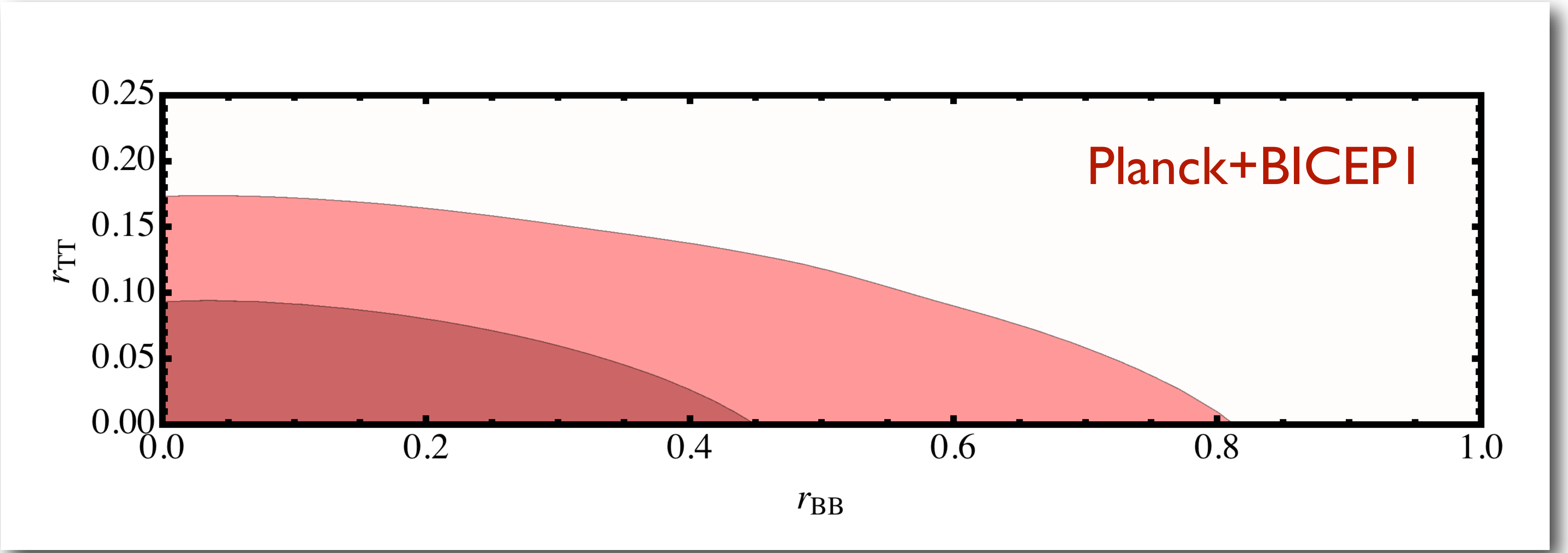

Constraint dominated by temperature data

B-mode search

$\mathcal{L}(r_{TT}, r_{BB})$ after BICEP2

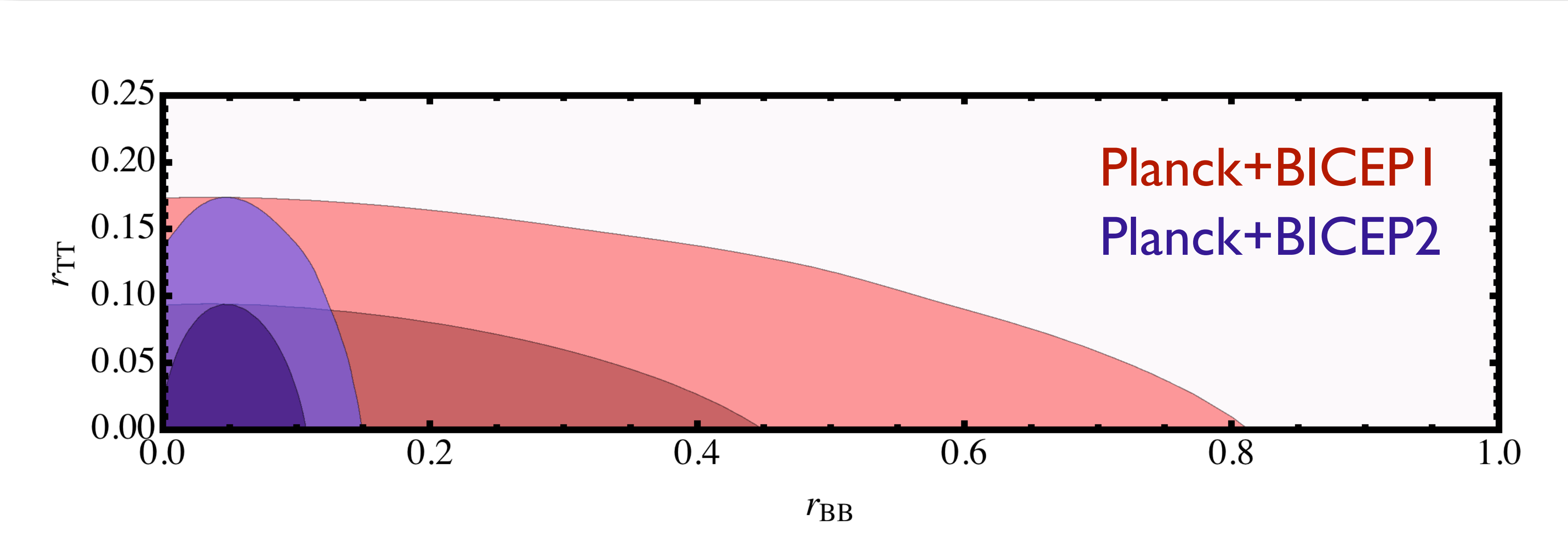

Constraint from polarization data comparable to constraint from temperature and will soon be significantly stronger.

B-mode search

$\mathcal{L}(r_{TT}, r_{BB})$ after BK14

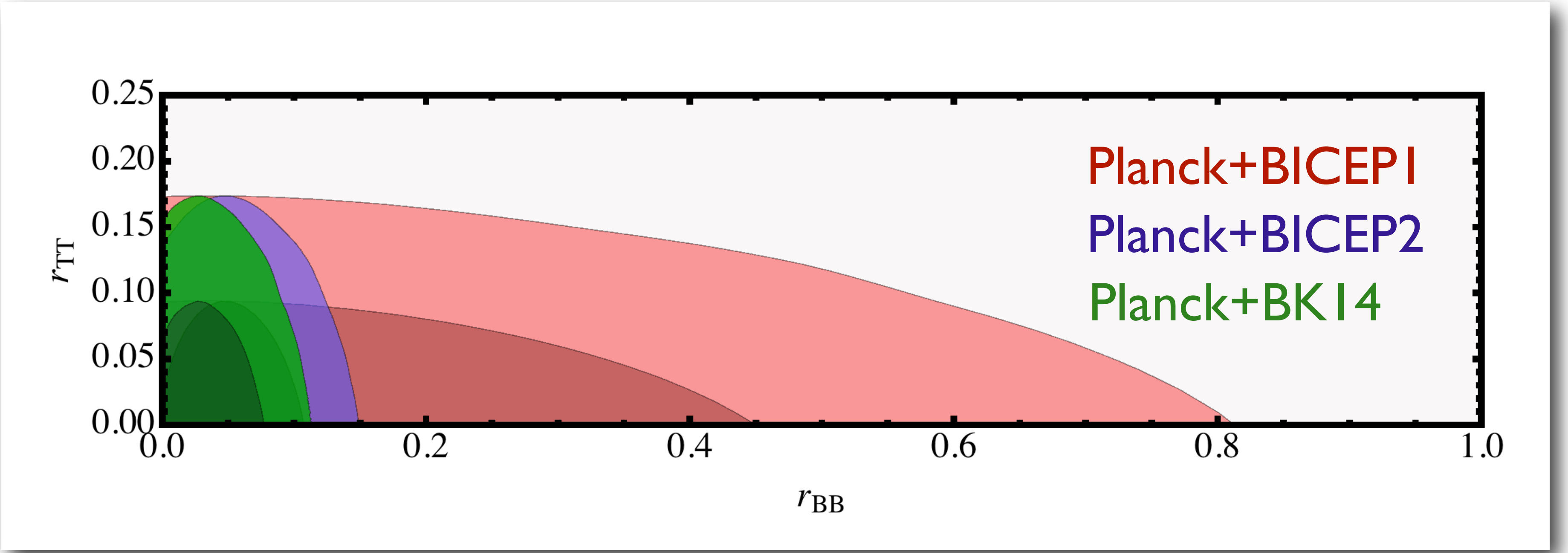

Constraint from polarization data comparable to constraint from temperature and will soon be significantly stronger.

Primordial B-modes

Stage III: now-2021

Primordial B-modes

Stage III.5: 2021-2026

http://simonsobservatory.org

- A five year, $45M+ program to pursue key Cosmic Microwave Background science targets, and advance technology and infrastructure in preparation for CMB-S4.

- Merger of the ACT and POLARBEAR/Simons Array teams.

- Tentative plans include:
  - Major site infrastructure
  - Technology development (detectors, optics, cameras)
  - Demonstration of new high throughput telescopes.
  - CMB-S4 class receivers with partially filled focal planes.
  - Data analysis

BERKELEY LAB · CONICYT · HEISING-SIMONS FOUNDATION · NSF · Penn · PRINCETON UNIVERSITY · SIMONS FOUNDATION

Primordial B-modes

Stage IV: 2026-2036

Potentially Space Missions

LiteBIRD, PICO

Primordial B-modes

- Seemingly straightforward because at linear order scalar perturbations do not generate B-modes.
- However, weak gravitational lensing of the CMB by intervening matter converts E- to B-modes
- Galactic foregrounds generate B-modes

Primordial B-modes

The challenge is to use maps with auto-spectra shown below to tell the difference between (r=0)...

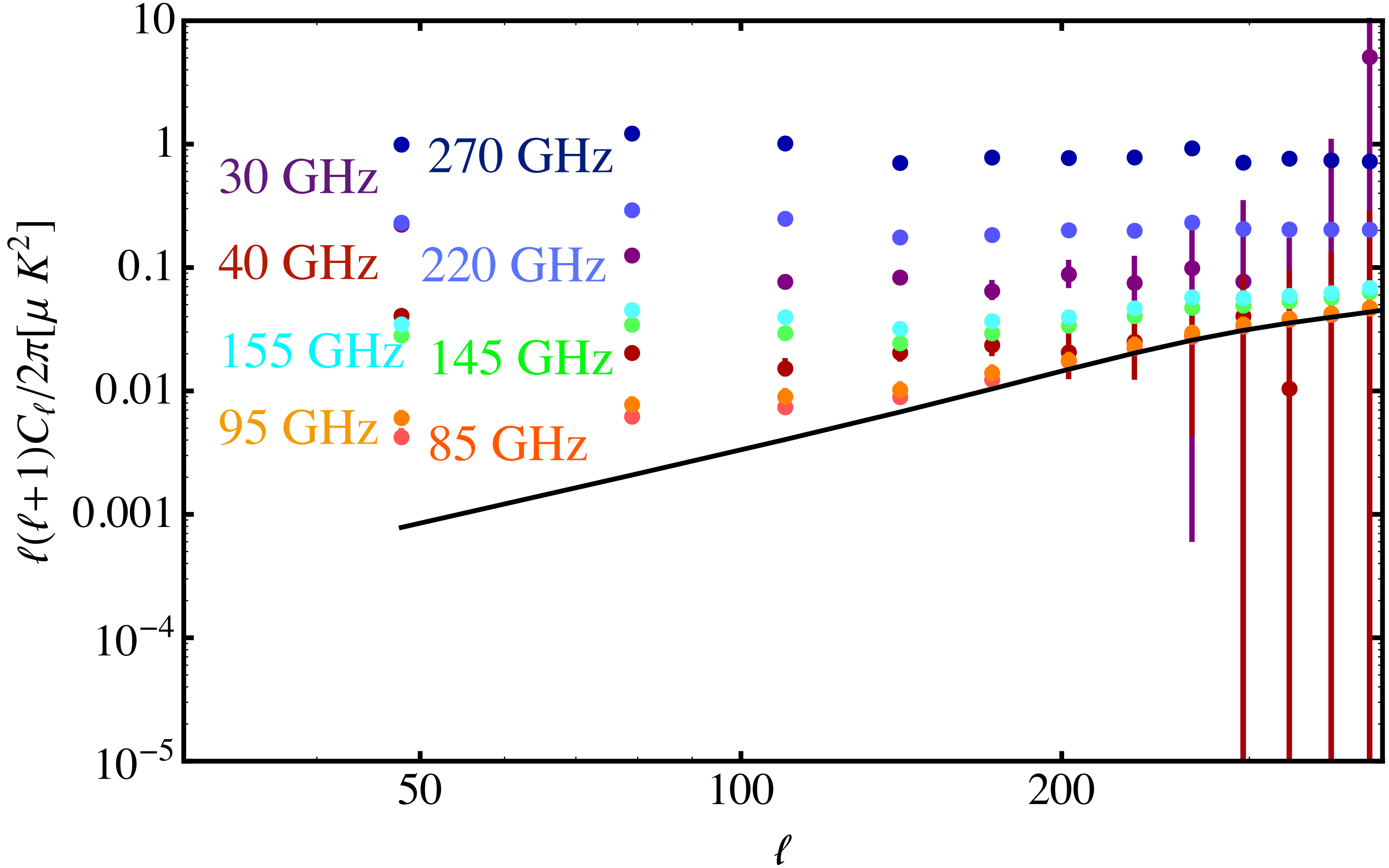

Primordial B-modes

and (r=0.003)...

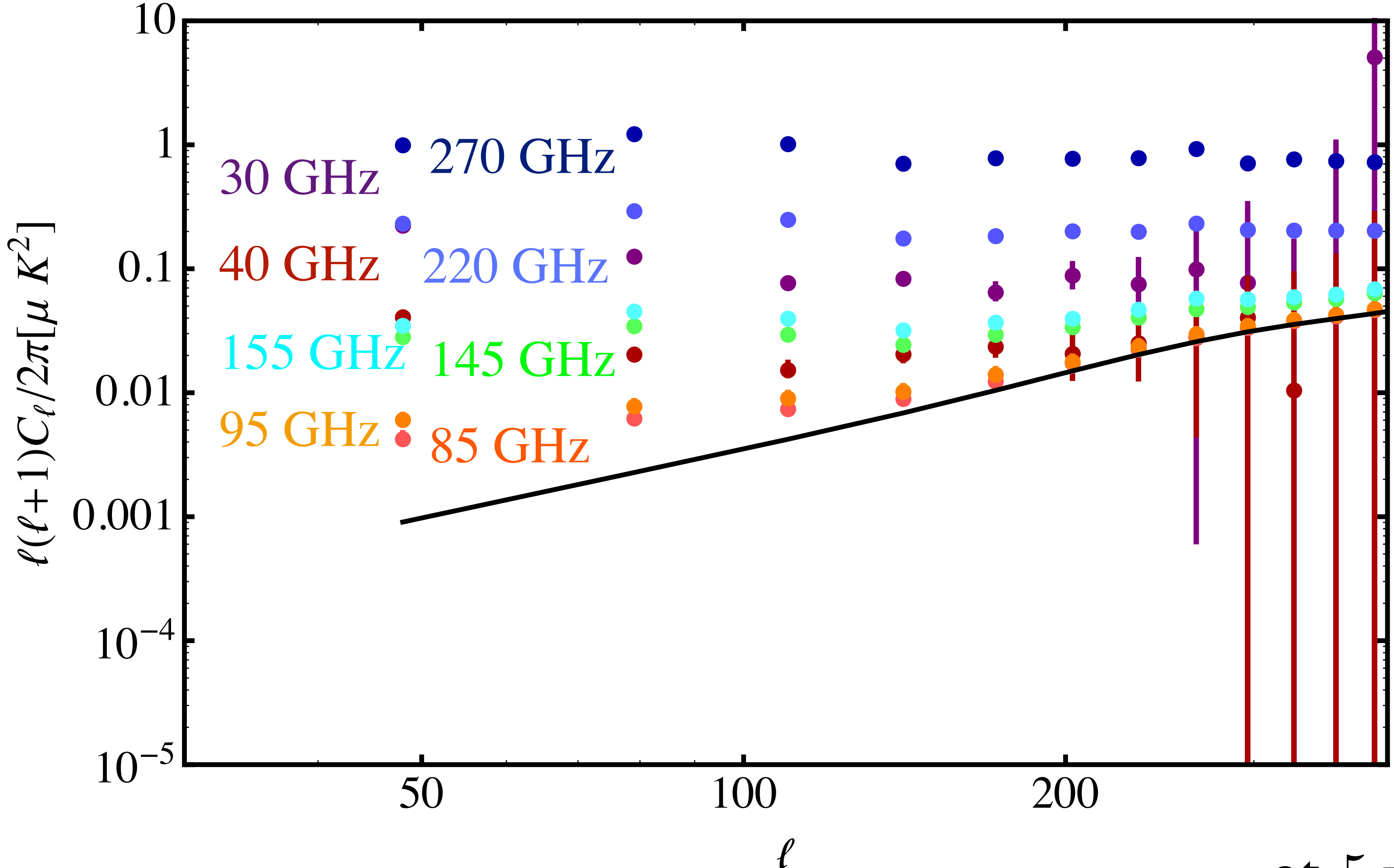

at 5σ

Primordial B-modes

Lensing B-modes can be partially removed through precise measurements of the lensing potential and E-modes

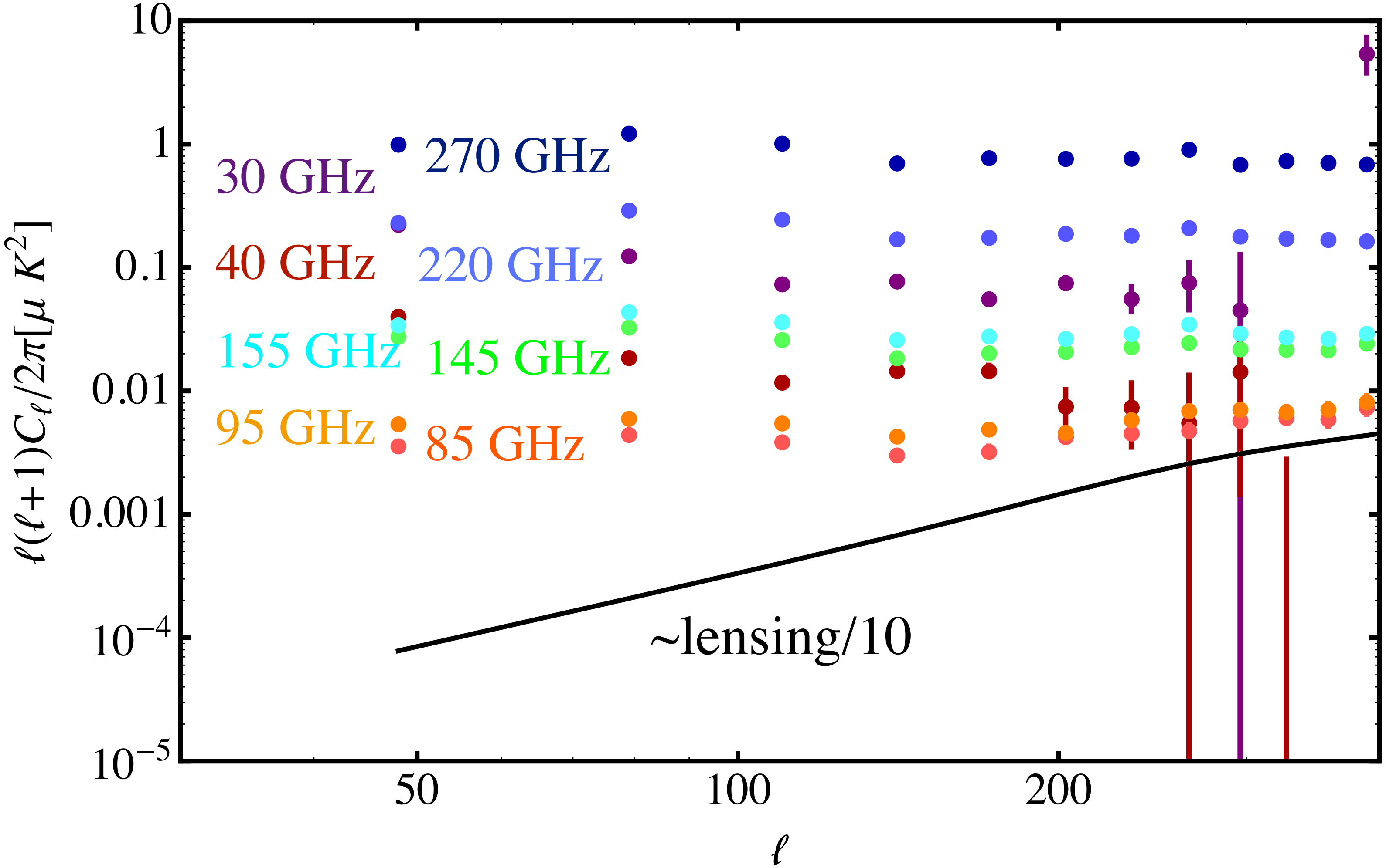

Primordial B-modes

r=0.003

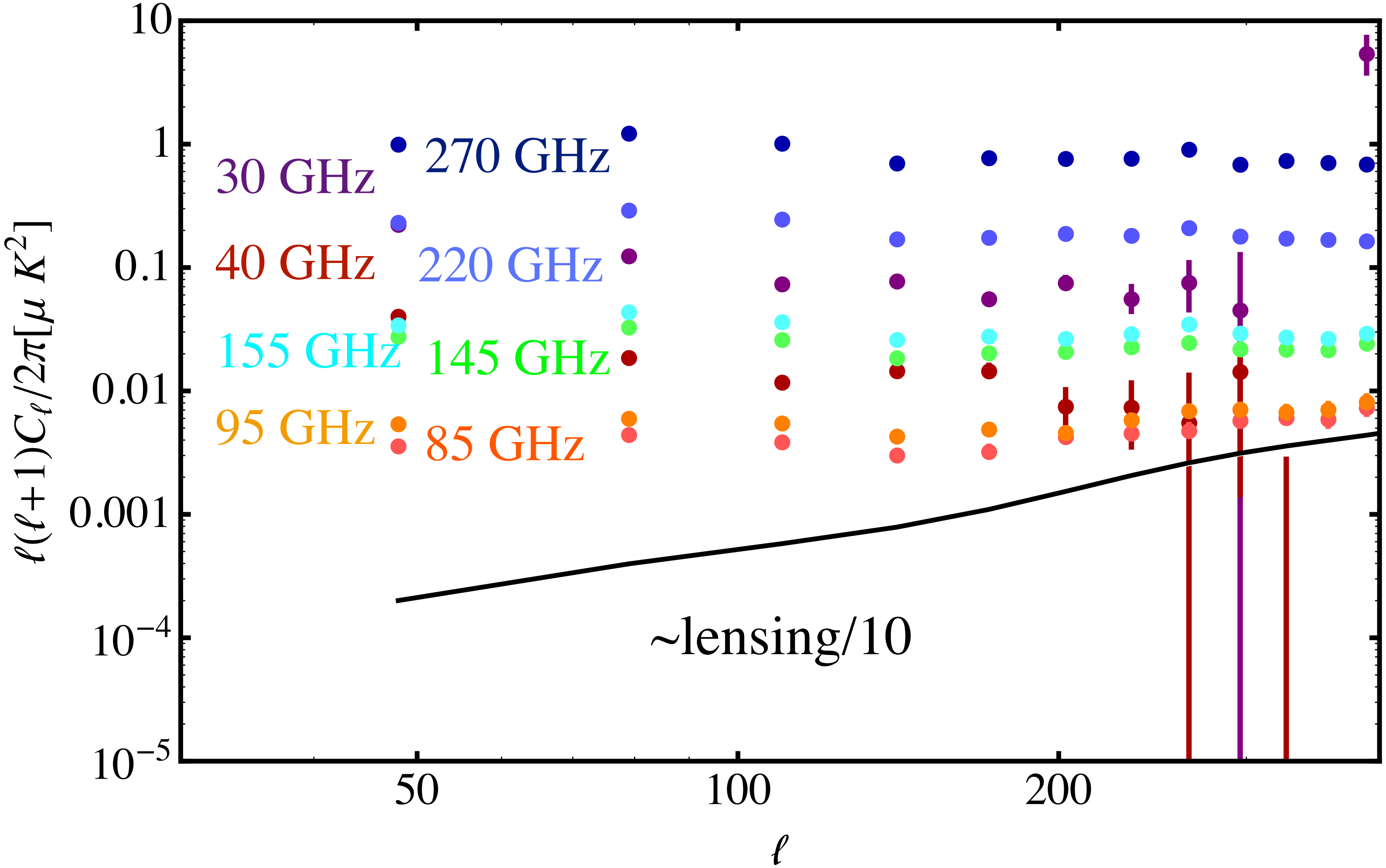

Primordial B-modes

Foreground cleaned spectrum and foreground residuals from simulation with r=0

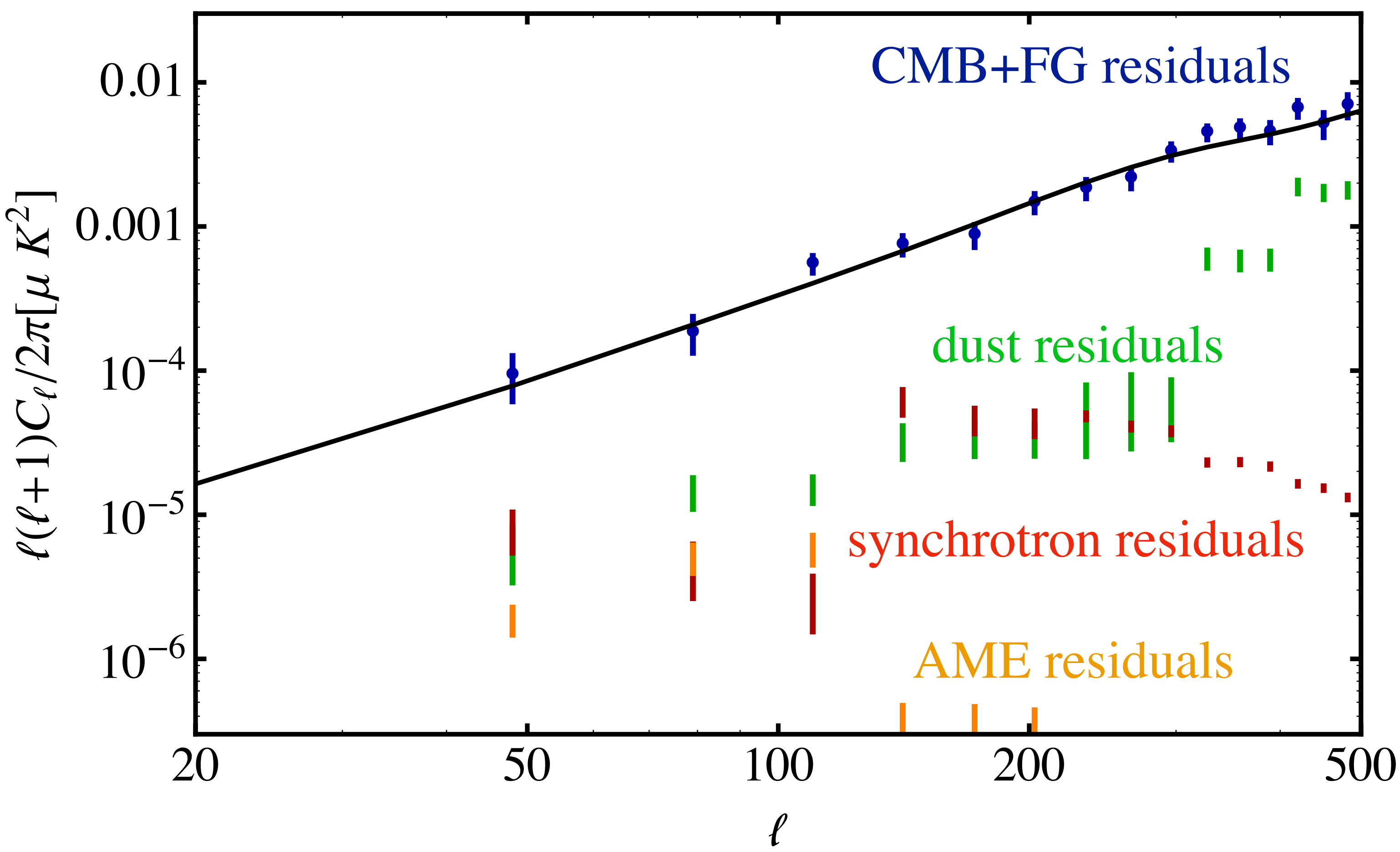

Primordial B-modes

CMB-S4 would detect r=0.01 at high significance

CMB-S4 Science Book (http://www.cmbs4.org)

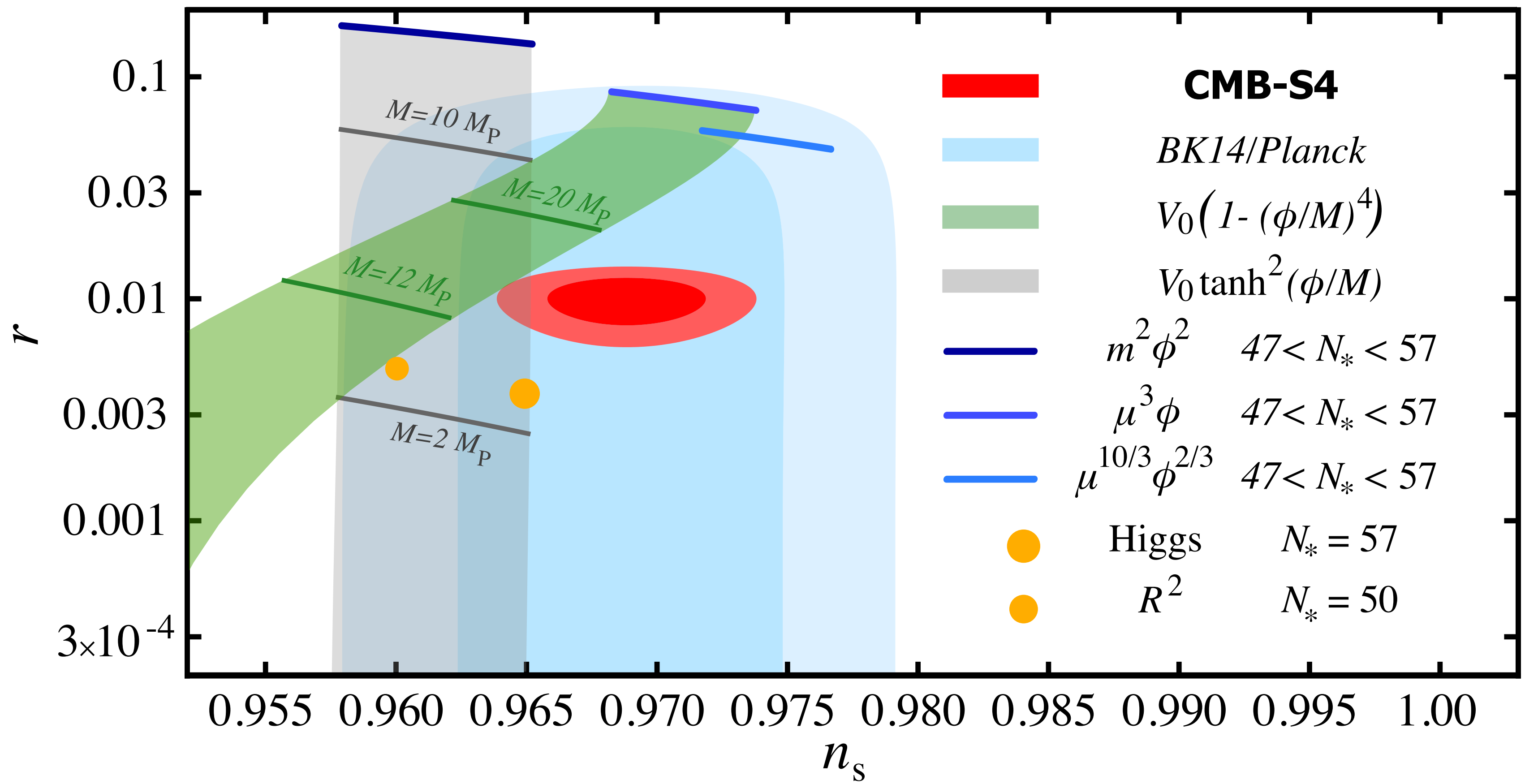

Primordial B-modes

Potential of a future space mission

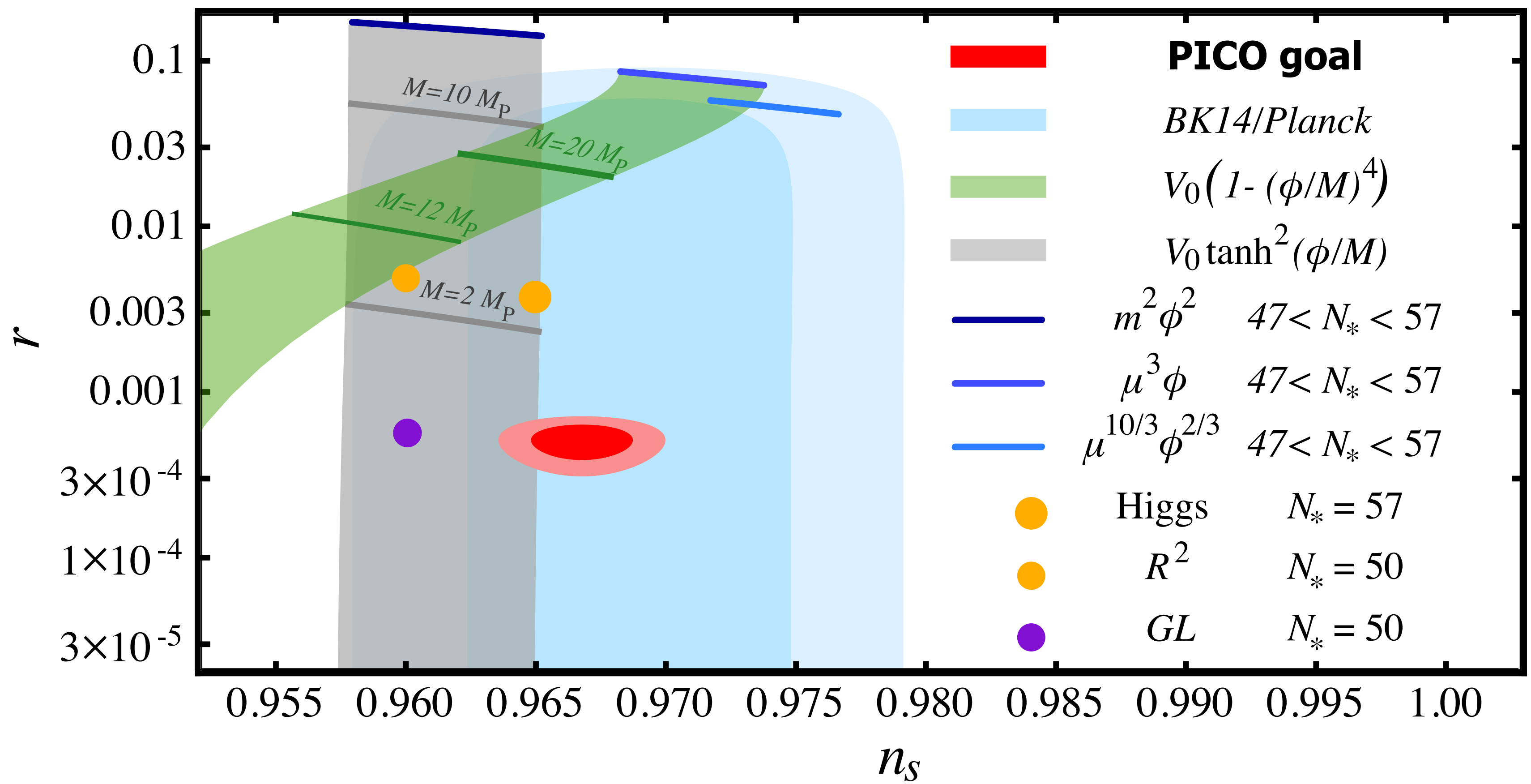

Primordial B-modes

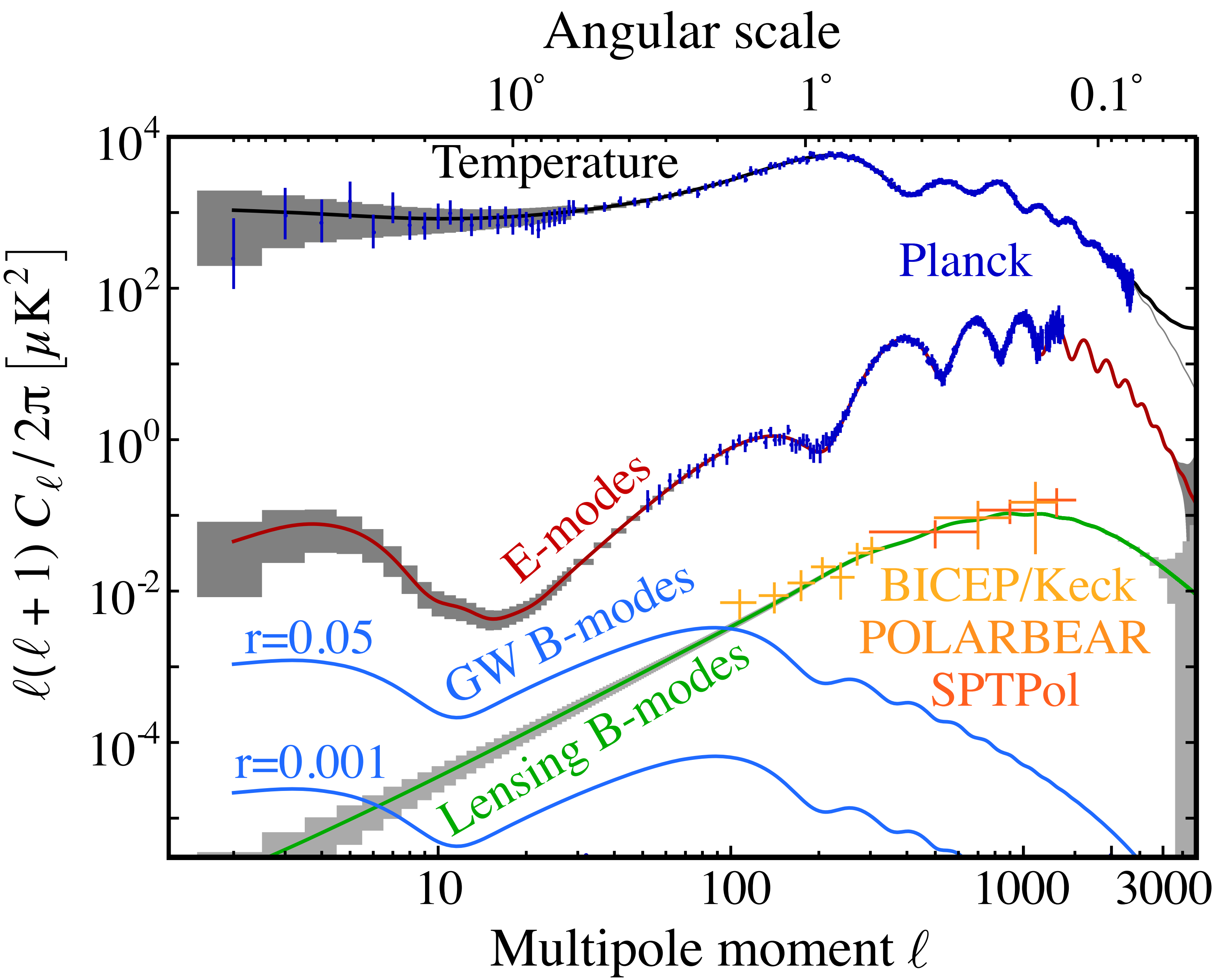

Conclusions

- The CMB has provided us with valuable information about the early universe for 53 years and will continue to do so for at least another decade.
- We may detect primordial gravitational waves, will measure neutrino masses, the number of effective relativistic degrees of freedom, ...
- Large scale structure surveys will provide a useful counter part
- The next decade should be very interesting in cosmology
- I hope you you enjoyed the lectures, know slightly more about the CMB than you did before, and perhaps play with the data.

Thank you